ALA-mediated Photodynamic Therapy
&
Delivery of Genes by Novel Polymers

by

Gözde Demirci

A Dissertation Submitted to the
Graduate School of Sciences and Engineering
in Partial Fulfillment of the Requirements for
the Degree of

Master of Science

in

Material Science and Engineering

August 18, 2020

ALA-mediated Photodynamic Therapy and Delivery of Genes by Novel Polymers

Koç University

Graduate School of Sciences and Engineering

This is to certify that I have examined this copy of a master's thesis by

Gözde Demirci

and have found that it is complete and satisfactory in all respects,
and that any and all revisions required by the final
examining committee have been made.

Committee Members:

_____

Prof. Dr. Havva Yağcı Acar (Advisor)

_____

Prof. Dr. Duygu Avcı Semiz

_____

Asst. Prof. Safacan Kölemen

Date: _____

Dedicated to my family…

ABSTRACT

ALA-mediated Photodynamic Therapy and Delivery of Genes by Novel Polymers

Gözde Demirci

Master of Science in Material Science and Engineering

August 18, 2020

Cancer is a challenging and complex disease to treat. Conventional therapeutic approaches, namely chemotherapy, radiotherapy and surgery, has limited success. Alternative treatment methods such as local phototherapies and gene therapy are highly promising in the treatment of different cancers as a single treatment modality or combination with conventional methods. In this thesis, *in vitro* studies for photodynamic therapy and its combination with chemotherapy for the treatment of colorectal cancer and bone targeting polyplexes made by novel copolymers for gene-therapy of osteosarcoma are described.

Photodynamic therapy (PDT) is a local, approved and promising approach in the treatment of cancer and bacterial infections. It induces tumor cell death creating reactive oxygen species (ROS), such as singlet oxygen, by photosensitizer excitation at a specific wavelength. It can be applied alone or in combination with other therapeutic techniques such as photothermal therapy (PTT) or chemotherapy for the treatment of colorectal, head, neck and breast cancer. Combination of chemotherapy and photodynamic therapy enhances therapeutic efficiency overcoming multidrug resistance (MDR) at low drug doses.

5-Aminolevulinic acid (ALA), a well-known and FDA approved photosensitizer, is a promising prodrug with the strong fluorescence for diagnosis and fast accumulation in the tumor tissue. ALA is produced in mitochondria as a rate-limited step of the heme biosynthesis pathway and converted to protoporphyrin IX (PpIX), which is a photosensitizer. For efficient PDT, exogenous ALA administration is needed to increase the PpIX concentration to therapeutic levels in the tumor cells.

In the first chapter of this thesis, ALA-mediated PDT and its combination with 5FU in the treatment of colorectal cancer is (HCT116 cells) described. Colorectal cancer is the 3rd most diagnosed tumor type and difficult to treat. Dose dependence of PDT, irradiation protocol and suitable cytotoxicity assays were first determined in 2D cell cultures and then applied to 3D early and late tumor models that are more realistic models to predict

the efficiency of the treatment. Alamar Blue was determined as the more appropriate method to evaluate *in vitro* toxicity, 100 µM ALA concentration and 10 min irradiation with blue lamp were found as an effective treatment for effective PDT in 2D and 3D. Besides, PpIX accumulation was significantly increased with an increase in the complexity of cell structures from 2D to late 3D cultures. As a result, ALA-mediated PDT causing apoptotic/necrotic death of HCT116 colorectal cancer cells in 3D tumor models was demonstrated. It was also noticed that ALA to PpIX conversion is hindered with the co-existence of 5FU; therefore, the 1/0.15 mol ratio of ALA/5FU was suggested as a promising recipe for combination therapy.

Osteosarcoma is aggressive bone cancer, whose treatment has not changed significantly for the past few decades. Although gene therapy has emerged as a potential treatment route, the need for efficient and non-toxic gene delivery systems targeting osteosarcoma cells remains a challenge. High molecular weight poly (ethyleneimine)s (PEIs), are used as universal transfection agents, however, cause significant cytotoxicity. On the other hand, poly (amidoamine)s (PAAs) are biocompatible, biodegradable Polymers with promising transfection efficiency.

In the second chapter, *in vitro* transfection of osteosarcoma cells with PEI-PAA copolymers with (bis)phosphonic acid groups with the potential to target bone is discussed. A set of novel polymers (PAEI) comprised of low molecular weight branched PEI (Mw = 1800 Da) and PAA macromers which were functionalized in different ratios with 5-amino-1-pentanol (AP) and (bis)phosphonic acid groups were studied. The PAEI polymers synthesized by the group of Prof. Duygu Avcı Semiz were tested on an osteosarcoma cell line (U-2 OS cells), which is one of the hardest cell types to transfect, and on muscle cells (C2C12 cells) as the control. The cytotoxicity and transfection efficiency of PAEIs were adjusted by altering the ratios of phosphonic acid (via APA, aminophosphonic acid) or bisphosphonic acid (via ALE, an amino bisphosphonic acid) content. The highest transfection efficiency was obtained with ALE containing PAEIs. The presence of PAA, PEI and ALE seemed to play a synergistic effect in the transfection performance of PAEIs. The most efficient PAEI polymer, containing a 0.7: 0.3 AP: ALE ratio, displayed a transfection efficiency that was 5-times higher than 25 kDa bPEI. This novel set of polymers can be promising candidates for the gene therapy of osteosarcoma.

ÖZETÇE

ALA-Aracılı Fotodinamik Terapi ve Genlerin Özgün Polimerler ile Taşınması

Gözde Demirci

Malzeme Bilimleri ve Mühendisliği, Yüksek Lisans

18 Ağustos 2020

Kanser, tedavisi zor ve karmaşık bir hastalıktır. Geleneksel terapötik yaklaşımlar, yani kemoterapi, radyoterapi ve cerrahi sınırlı başarıya sahiptir. Lokal fototerapiler ve gen terapisi gibi alternatif tedavi yöntemleri, tek bir tedavi yöntemi veya geleneksel yöntemlerle kombinasyon halinde farklı kanserlerin tedavisinde oldukça ümit vericidir. Bu tezde, fotodinamik terapi için in vitro çalışmalar ve bunun kolorektal kanser tedavisi için kemoterapi ile kombinasyonu ve osteosarkomun hedefli gen tedavisi için yeni kopolimerler ile yapılan gen transfeksiyon çalışmaları yer almaktadır.

Fotodinamik tedavi (PDT), kanser ve bakteriyel enfeksiyonların tedavisinde yerel, onaylanmış ve ümit verici bir yaklaşımdır. Belirli bir dalga boyunda fotohassaslaştırıcıların uyarımı ile tekli oksijen gibi reaktif oksijen türleri (ROS) oluşturarak tümör hücresi ölümünü indükler. Kolorektal, baş, boyun ve meme kanserinin tedavisi için tek başına veya fototermal terapi (PTT) veya kemoterapi gibi diğer terapötik tekniklerle kombinasyon halinde uygulanabilir. Kemoterapi ve fotodinamik tedavinin kombinasyonu, düşük ilaç dozlarında çoklu ilaç direncini (MDR) kırarak terapötik etkinliği arttırır.

İyi bilinen ve FDA onaylı bir fotohassaslaştırcı olan 5-aminolevulinik asit (ALA), tümör dokusundaki floresansı ile tanı, PDT etkisiyle tedavi için umut veren bir ön ilaçtır. ALA, mitokondride hem-biyosentez yolunun hız sınırlı bir adımı olarak üretilir ve bir fotosensitizör olan protoporfirin IX'a (PpIX) dönüştürülür. Etkili PDT için, tümör hücrelerindeki PpIX konsantrasyonunu terapötik seviyelere yükseltmek için eksojen ALA uygulamasına ihtiyaç vardır.

Bu tezin ilk bölümünde, kolorektal kanser tedavisinde ALA aracılı PDT ve bunun 5-florourasil (5FU) ile kombinasyonu (HCT116 hücreleri) anlatıldı. Kolorektal kanser, en çok teşhis edilen 3. tümör türüdür ve tedavisi zordur. PDT'nin doz bağımlılığı, ışınlama protokolü ve uygun sitotoksisite deneyleri önce 2D hücre kültürlerinde belirlendi ve ardından tedavinin etkinliğini tahmin etmek için daha gerçekçi modeller olan 3D erken ve geç tümör modellerine uygulandı. Alamar Blue, in vitro toksisiteyi değerlendirmek için uygun bir yöntem olarak belirdi. 100 µM ALA konsantrasyonu ve mavi lamba ile 10

dakika ışınlamanın, 2D ve 3D hücre çalışmalarında etkin bir PDT yarattığı gösterildi. Ayrıca, hücre yapılarının karmaşıklığında 2D'den geç 3D kültürlere geçildiğinde PpIX birikimi önemli ölçüde arttı. Sonuç olarak, 3D tümör modellerinde HCT116 kolorektal kanser hücrelerinin apoptotik / nekrotik ölümüne neden olan ALA aracılı PDT ile yok edilebildiği gösterildi. Ayrıca ALA'nın PpIX'e dönüşümünün 5FU'nun varlığıyla engellendiği de fark edildi; bu nedenle, ALA / 5FU'nun 1 / 0.15 mol oranı, kombinasyon tedavisi için umut verici bir reçete olarak önerildi.

Osteosarkom, tedavisi son yirmi yıldır önemli ölçüde değişmeyen agresif kemik kanseridir. Gen terapisi potansiyel bir tedavi yolu olarak ortaya çıkmış olsa da, osteosarkom hücrelerini hedefleyen verimli ve toksik olmayan gen sağlama sistemlerine duyulan ihtiyaç bir zorluk olmaya devam etmektedir. Yüksek moleküler ağırlıklı poli(etilenimin) (PEI) evrensel transfeksiyon ajanları olarak kullanılır, ancak önemli sitotoksisiteye neden olur. Öte yandan, poli(amidoamin)`ler (PAA'lar), ümit verici transfeksiyon verimliliği ile biyolojik olarak uyumlu, biyolojik olarak parçalanabilen yeni polimerlerdir.

İkinci bölümde, osteosarkom hücrelerinin kemiği hedefleme potansiyeline sahip (bis)fosfonik asit grupları içeren PEI-PAA kopolimerleriyle in vitro transfeksiyonu tartışılmaktadır. Düşük moleküler ağırlıklı dallanmış PEI (Mw = 1800 Da) ve 5-amino-1-pentanol (AP) ve (bis)fosfonik asit grupları ile farklı oranlarda işlevselleştirilmiş PAA makromerlerinden oluşan bir dizi yeni polimer (PAEI) üzerinde çalışıldı. Prof. Duygu Avcı Semiz grubu tarafından sentezlenen PAEI polimerleri, transfekte edilmesi en zor hücre türlerinden biri olan osteosarkom hücre çizgisinde (U-2 OS hücreleri) ve kontrol olarak kas hücrelerinde (C2C12 hücreleri) test edildi. PAEI'lerin sitotoksisitesi ve transfeksiyon etkinliği, fosfonik asit (APA yoluyla, aminofosfonik asit yoluyla) veya alendronat (ALE, bir amino bifosfonik asit yoluyla) oranlarını değiştirerek ayarlandı. En yüksek transfeksiyon verimi PAEI içeren ALE ile elde edildi. PAA, PEI ve ALE'nin varlığının, PAEI'lerin transfeksiyon performansında sinerjistik bir etki yarattığı göründü. 0.7: 0.3 AP: ALE oranı içeren en verimli PAEI polimeri, 25 kDa bPEI'den 5 kat daha yüksek bir transfeksiyon etkinliği gösterdi. Bu yeni polimer seti, osteosarkomun gen terapisi için umut verici adaylar olabilir.

ACKNOWLEDGEMENTS

First of all, I would like to express my sincere gratitude to my advisor, Prof. Dr. Havva Funda Yağcı Acar. I am grateful for all the opportunities that she has provided since the beginning of my lab days. It has been a privilege for me to study under her guidance.

I would like to thank Prof. Dr. Duygu Avcı Semiz and Asst. Prof. Safacan Kölemen for being on my thesis committee and for their valuable contributions.

I would like to express my appreciation to Dr. Yeliz Utku Konca ve Assoc. Prof. Uğur Ünal for supporting my laboratory experience during my undergraduate and graduate studies.

I am deeply grateful to my dear Dr. Fatma Demir Duman and Pelin Turan Buz for teaching me the nanomaterial world. I sincerely thank Dr. Kübra Bilici and Dr. Özge Çavuşlar for their support, encouragement and help in both experimental work and in life. I am thankful to previous and current members of Polymers and Nanomaterials Research Group.

I especially thank Prof. Dr. Alexander J. MacRobert, Prof. Dr. Marilena Loizidou and Dr. Layla Mohammad-Hadi from the University College London for their help in PDT and 3D studies during my visit to London and their support throughout the project. I would like to thank Melek Naz Güven and Seçkin Altuncu from Boğaziçi University for their valuable polymers and friendship during my MS studies. Also, I am thankful to Dr. Buse Cevatemre and Batuhan Kalkan from KUTTAM for their help and guidance in plasmid isolation and transfection procedure.

I would like to deeply thank my family: my grandparents Ayşe and Hüseyin Demirci, my mother Ayşe Demirci, my father Tevfik Demirci and my sister Tuğçe Demirci Atam and her husband Serkan Atam for their unconditional support, love, guidance and trust. I could not succeed in this MS program without them.

There is always a special person in these stressful times to talk and laugh together. I want to thank that person, Duhan Kurt, for her true friendship and endless support.

Table of Contents

List of Tables

List of figures

Abbreviations

2D – 3D	2-3 dimensional
5FU	5-fluorouracil
AB	Alamar Blue
AK	Actinic keratosis
ALA	5-Aminolevulinic acid
ALAS	Aminolevulinic acid synthase
ALE	Alendronate
AP	5-amino-1-pentanol
APA	2-aminoethyl phosphonic acid
ATCC	American Type Culture Collection
BC	British Council
BCC	Basal cell carcinoma
BD	Becton Dickinson
BP	Bisphosphonate
bPEI	Branched poly (ethyleneimine)
BSA	Bovine serum albumin
C2C12	Mouse myoblast muscle cell line
CoA	Coenzyme A
Da	Dalton
DAPI	4’,6-diamidino-2-phenylindole
DCF	2’,7’-Dichlorofluorescein
DCF-DA	2’,7’-Dichlorofluorescin diacetate
DLS	Dynamic Light Scattering
DMEM	Dulbecco’s modified Eagles medium
DMSO	Dimethyl sulfoxide
DNA	Deoxyribonucleic acid
ECM	Extracellular matrix
EDTA	Ethylenediamine tetra acetic acid
ER	Endoplasmic reticulum
FACS	Fluorescence-activated cell sorting
FBS	Fetal bovine serum
FDA	Food and Drug Administration
FITC	Fluorescein isothiocyanate
GFP	Green fluorescence protein
HCT116	Human colon cancer cell line
HEPES	(4-(2-hydroxyethyl)-1-piperazineethanesulfonic acid)
HT-29	Human colorectal adenocarcinoma cell line
IC50	Half maximal inhibitory concentration
KU	Koc University
LED	Light-emitting diode
lPEI	Linear poly (ethyleneimine)
MDR	Multidrug resistance
MEM	Minimum Essential Medium
MTT	Thiazolyl blue tetrazolium bromide
OS	Osteosarcoma
PAA	Poly (amidoamine)
PAEI	Poly (amido ethyleneimine)
PBS	Phosphate buffered saline
PDI	Polydispersity index

PDT	Photodynamic Therapy
PEG	Polyethylene glycol
Pen/strep	Penicillin/streptomycin
PI	Propidium iodide
PpIX	Protoporphyrin IX
PS	Photosensitizer
ROS	Reactive oxygen species
SD	Standard deviation
TETA	Triethylenetetramine
TUBITAK	Scientific and Technological Research Council of Turkey
U-2 OS	Bone osteosarcoma epithelial cell line
UCL	University College London
UV	Ultraviolet

Chapter 1: 5-Aminolevulinic Acid-Mediated Photodynamic Therapy Introduction

1.1 Photodynamic Therapy

Photodynamic therapy (PDT) is a highly promising and minimally invasive light-based therapeutic approach for treating various types of cancers, such as lung cancers (Pramual et al., 2020), breast cancers (Li et al., 2020), head and neck tumors (Bredell, Besic, Maake, & Walt, 2010) and colorectal cancers (Dolmans, Fukumura, & Jain, 2003). Photosensitization started to draw attention in various research fields in the 1900s (Dolmans et al., 2003). PDT was used mainly in dermatology due to its safety and accessibility to the light, unlike inner parts of the body in 1999 (Gold & Goldman, 2004).

Nowadays, PDT is extensively studied in oncology (Dolmans et al., 2003). PDT attracted a significant attention because of its locality, high selectivity, and recovery with a small scar or no scar (Triesscheijn, Baas, Schellens, & Stewart, 2006; Wachowska et al., 2011). By exciting photosensitizer at an appropriate wavelength with various light sources, tumor cell death is induced due to the accumulation of reactive oxygen species (ROS) at the irradiated tumor site (Dougherty, Gomer, & Henderson, 1998). PDT induces cellular death because of apoptosis, necrosis and/or autophagy. PDT is highly efficient in the treatment of tumors due to vascular shutdown and local inflammatory reaction (Wachowska et al., 2011).

The photosensitizers (PS) are special light absorbers and emit light at a specific wavelength (Oleinick, 2011). The difference of photosensitizers from the other light-absorbing molecules is the efficiently populated excited triplet states which increase the probability of reacting with other molecules, particularly oxygen molecules (Oleinick, 2011). Photosensitizers are inactive and non-toxic molecules in the absence of light which provides safe treatment in PDT and limits off-site toxicity in the non-irradiated tissue (Wachowska et al., 2011). PS are excited to higher energy states when interacting with light (Dolmans et al., 2003). Then, this energy can be transferred to intracellular oxygen to generally produce free radicals/ singlet oxygen or can be released as fluorescence or phosphorescence emissions (Figure 1.1).

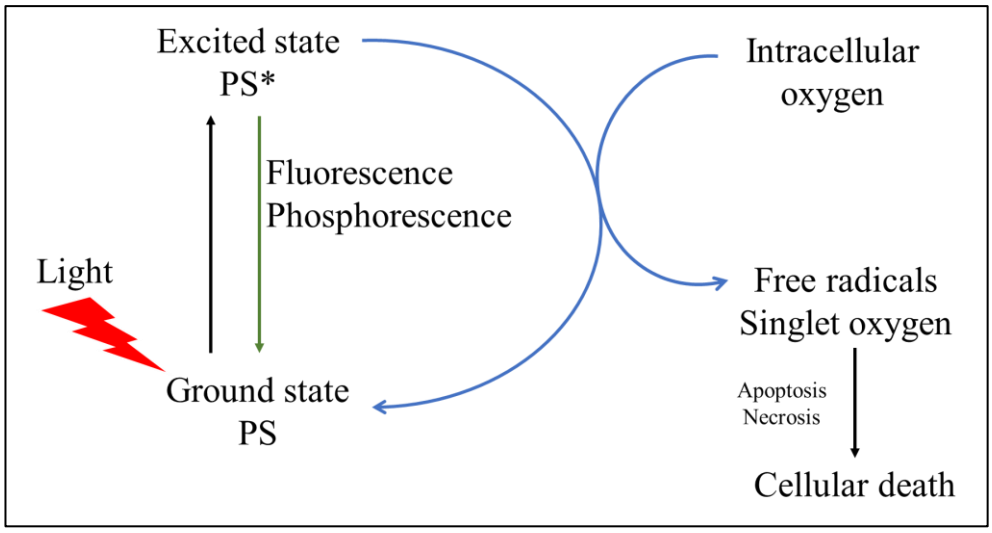

Figure 1.1. The mechanism of photodynamic therapy (PDT).

The photosensitizer is excited with light energy from the lower energy level (ground state) to a higher energy level (excited state) (Buettner, 2013; Mroz, Yaroslavsky, Kharkwal, & Hamblin, 2011). The excited photosensitizer is subjected to two types of photosensitization, called Type I and Type II (Figure 1.2) (Oleinick, 2011). In Type I, excited PS undergoes a chemical reaction with other biological substances and produces radicals. In most cases, excited PS takes an electron from the surrounding substances. The produced anionic PS radicals react with a triplet state of the intracellular oxygen molecule. Type I photosensitization ends with the formation of reactive oxygen species (ROS), such as superoxide and peroxide. In Type II, the energy of excited PS is directly transferred to a ground state of the oxygen molecule to form singlet oxygen. By reacting with electron-rich crucial molecules, such as NADH, cystine, guanine bases of DNA and RNA, singlet oxygen causes irreversible damage in cancerous cells (Bhawalkar, Kumar, Zhao, & Prasad, 1997; Oleinick, 2011). In both types, intracellular oxygen is vital whether in the reaction with the anionic PS radicals in Type I or the direct energy transfer from the excited PS in Type II (Figure 1.3) (Oleinick, 2011).

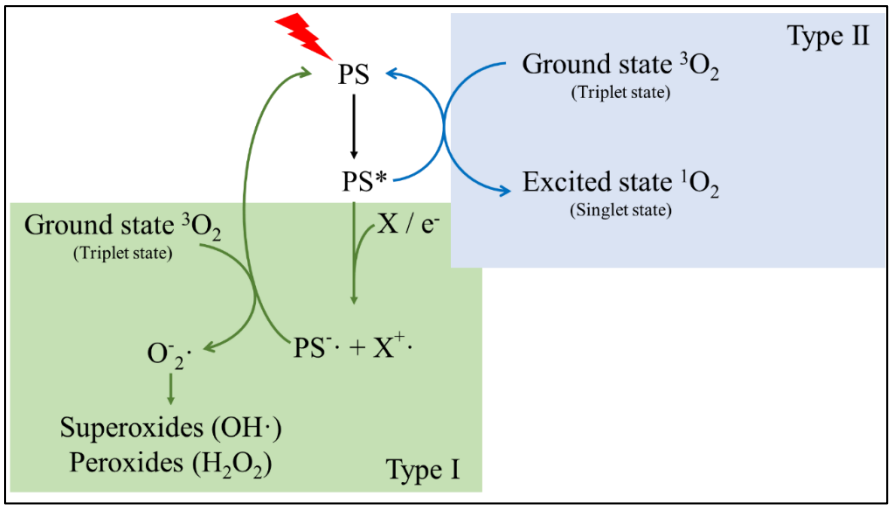

Figure 1.2. The mechanism of Type I and Type II photosensitizations.

Photosensitizers are mostly retained by malignant tumor cells rather than normal cells (Loschenov, Konov, & Prokhorov, 2000; Oleinick, 2011). Due to the altered metabolism of the cancer cells in both heme biosynthesis and mitochondrial activity, these agents are highly accumulated in tumors. They offer an opportunity for a combination of diagnosis and therapy at the same time (Dougherty et al., 1998; Inoue et al., 2009; Yang, Palasuberniam, Kraus, & Chen, 2015). Diagnosis of tumor tissue is essential in oncology, and may be achieved with such photosensitizers that luminesce as well (Bunke et al., 2000; Dougherty et al., 1998; Inoue et al., 2009). The high selectivity of photosensitizers increases the efficiency of PDT and local cancer treatment with minimal side effects of treatment on the healthy tissue.

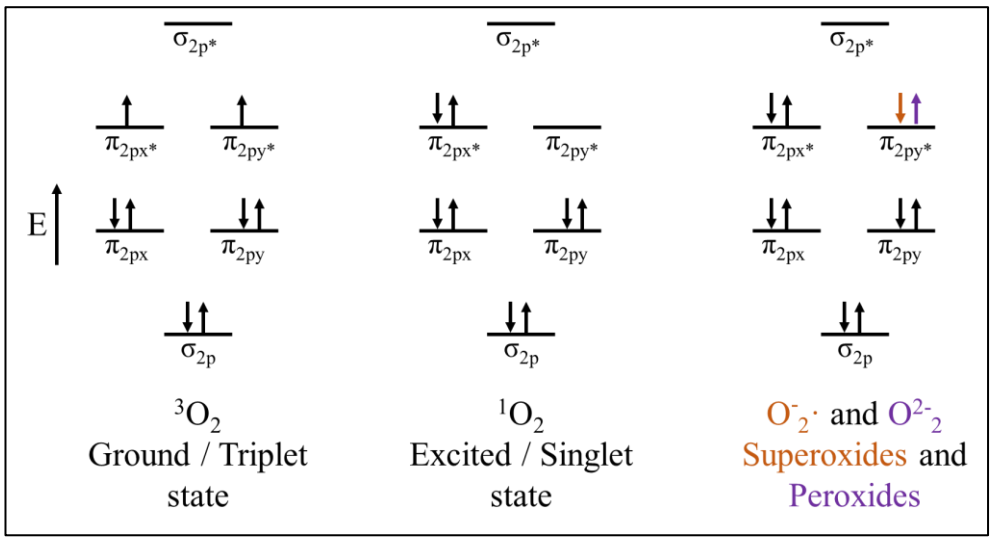

Figure 1.3. Molecular orbital diagrams of triplet and singlet states of oxygen and some reactive oxygen molecules.

Porphyrins are well-known photosensitizers and are commonly used in clinical cancer phototherapies (Figure 1.4). Porphyrins are naturally produced in mitochondria of cells with the heme metabolic pathway, but excess amounts are need for therapy, hence exogenous porphyrins are administrated for PDT. PS accumulation can be observed in various organelles, such as mitochondria and ER (Mroz et al., 2011; Wachowska et al., 2011). After the irradiation, this accumulation leads to cell death pathways (Mroz et al., 2011). All photosensitizers may be considered as prodrugs since they are inactive until the illumination and are discarded from the body without causing significant damage.

For the activation of the PS, laser systems, halogen lights and LEDs are used (Juzeniene, Juzenas, Ma, Iani, & Moan, 2004; Loschenov et al., 2000). When lasers are used, the power of the laser should be kept low to prevent the tissue heating and related necrosis of the tissue and the skin (Loschenov et al., 2000). Also, the transfer of the light with an optical fiber mostly reduces the power and controls the delivery light intensity (Triesscheijn et al., 2006). LEDs are commonly used in clinical due to low power, simplicity of the devices, availability in a wide range of wavelengths and low cost (Triesscheijn et al., 2006). LEDs are preferred over halogen lights due to availability in specific wavelengths and lower heat dissipation (Juzeniene et al., 2004).

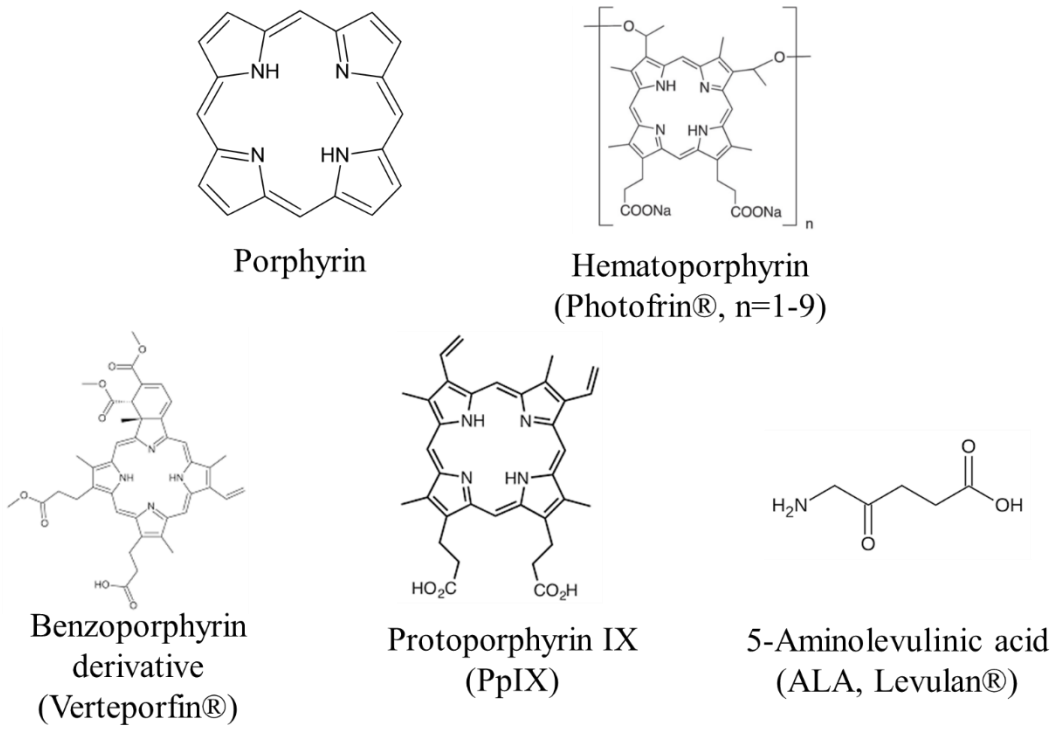

Figure 1.4. Chemical structures of some important porphyrin type of photosensitizers.

1.2 5-Aminolevulinic acid (ALA) Based PDT

All photosensitizers are administrated as a porphyrin derivative and directly react with light. However, ALA is a prodrug that is converted to porphyrin *in vivo* bypassing the limitations of porphyrin administration such as light sensitivity, hence is quite attractive in the clinic (Q. Peng et al., 1997). ALA is generally used in the treatment of actinic (solar) keratoses (AK) and basal cell carcinoma (skin tumor) (BCC) (Gold & Goldman, 2004; Kennedy, Marcus, & Pottier, 1996; Triesscheijn et al., 2006). In normal cell metabolism, ALA is a first and rate-limiting product from glycine and succinyl-CoA in mitochondria in the heme biosynthesis pathway (de Oliveira Silva et al., 2010; Kennedy et al., 1996; Loschenov et al., 2000; Yang et al., 2015). The formation of heme, integrated into hemoglobin (used in transportation of oxygen), controls the production of ALA using a feedback mechanism (Figure 1.5) (de Oliveira Silva et al., 2010). The altered heme biosynthesis and mitochondrial activity of the cancer tissue cause high protoporphyrin IX (PpIX) accumulation. Also, the exogenous ALA administration increases the accumulated PpIX concentration in the tumor cells, hence the efficiency of tumor-targeted PDT (Kennedy et al., 1996). ALA is a highly hydrophilic molecule which mostly causes penetration problems through the skin or cell membranes (Q. Peng et al., 1997; Rodriguez et al., 2006; Triesscheijn et al., 2006). In the physiological pH, ALA is mainly zwitterion which decreases the bioavailability and causes rapid clearance from the body (Triesscheijn et al., 2006; Wachowska et al., 2011). Due to low penetration and fast clearance of ALA, systemic administration of ALA decreases the PDT phototoxicity (Wachowska et al., 2011). Modification of the ALA with lipophilic molecules in the form of methyl ester or hexyl ester, for example, solves both penetration and clearance problems (Juzeniene et al., 2004; Rodriguez et al., 2006; Triesscheijn et al., 2006; Wachowska et al., 2011).

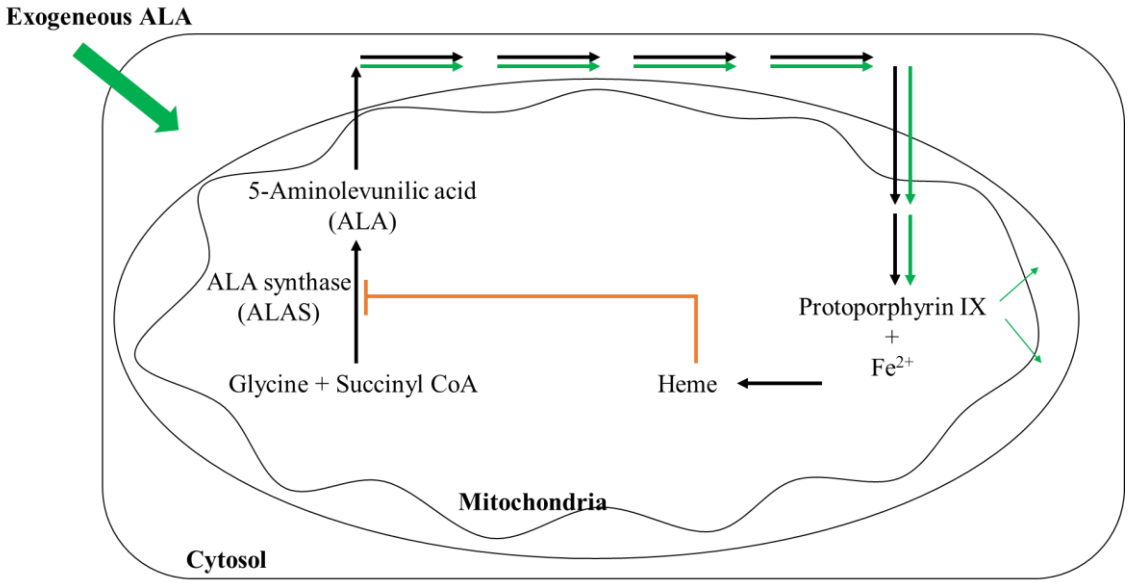

Figure 1.5. Heme biosynthesis and important steps in ALA mechanism.

Non-toxic and inactive photosensitizers are activated with light in PDT (Mroz et al., 2011). For a successful PDT, therapeutic dose of the PS should accumulate in the tumor before irradiation, hence the time between the administration of the PS and light irradiation is critical, as well as the duration of irradiation (Mroz et al., 2011; Yang et al., 2015). In clinical research, the time interval between PS administration and illumination is planned in short intervals for easy follow-ups of the trials. Also, the treatment time should be short for the comfort of patient (Allison et al., 2004). The rapid metabolism of topical ALA provides an advantage in fast accumulation in the target tissue, which is 4-6 hours in the clinic (Wachowska et al., 2011). Also, the light treatment of ALA accumulated tissue lasts 30 minutes or one hour (Gold & Goldman, 2004). ALA and derivatives are irradiated with both blue (400 nm) and red (630 nm) lights. The absorbance of ALA in the blue wavelength is more than the red, however, red is safer and provides deeper light penetration. The derivatives of ALA are activated with different wavelengths (Dolmans et al., 2003). The red illumination is preferred in methyl-ALA derivative, while the blue light is used in ALA and hexyl-ALA (Allison et al., 2004). In the most cases of ALA-mediated PDT, red light, specifically 630 nm, is preferred for the treatment of actinic keratoses and BCC (Dolmans et al., 2003; Gold & Goldman, 2004; Kennedy et al., 1996; Q. Peng et al., 1997). In the diagnosis of some cancers, such as the bladder, head and neck, and brain tumors, the blue light is used due to the high absorbance of ALA to generate the reddish luminescence (Dolmans et al., 2003).

Colorectal cancer is the third most common cancer and the fourth leading cause of cancer deaths worldwide (Rawla, Sunkara, & Barsouk, 2019). While 36% of cases are ending by death, 7% of deaths is younger than age 49 in the United States in 2020 (Siegel et al., 2020). The survival time after diagnosis is prolonged with some FDA approved drugs, such as fluorouracil and oxaliplatin (Meyerhardt & Mayer, 2005). However, like most other type of cancers, colorectal cancer shows resistance to chemotherapy, and hence significantly reduces the efficiency of the treatment (Ashrafizadeh et al., 2020; Borralho et al., 2009; De Angelis et al., 2004; Howells et al., 2011). For more effective treatment, combinations of different drugs or combination therapy such as chemotherapy combined with, gene therapy or PDT are being used in the clinic and/or under investigation (Ashrafizadeh et al., 2020; Borralho et al., 2009; de Freitas, Kimura, Rubira, & Muniz, 2020; Meyerhardt & Mayer, 2005). For (multi)drug resistant cancers, sensitization of cells with PDT is actively used as a combination therapy (Khdair et al., 2010; Li et al., 2020; Pramual et al., 2020).

In the treatment of colorectal cancer, ALA-based PDT combined with traditional chemotherapy agent 5-fluorouracil (5FU) may provide enhanced efficacy. This may be achieved by loading both agents to a nanoparticle designed to target colorectal cancer which is known to overexpress EGFR (endothelial growth-factor receptor). However, ALA-PpIX conversion is usually cell-type and time-dependent (Eskiler et al., 2020; Krieg, Messmann, Rauch, Seeger, & Knuechel, 2002; Wawrzyniec, Kawczyk-Krupka, Czuba, Krol, & Sieron, 2015). Hence, effective concentrations of ALA in the treatment of colorectal cancer cell lines and best procedures such as incubation time, dose, irradiation time as well as most sensitive methods to determine toxicity should be studied. Here, all these crucial studies were performed in 2D and 3D cell cultures, before going into more complex structures such as ALA and 5FU loaded targeted nanoparticles.

Traditionally, pre-clinical research of an anticancer drug is studied in 2D culture systems because 2D cell cultures are easy-to-use and give reliable results (Khot et al., 2018). However, 2D cell cultures fail to replicate the effects of the cell-cell and the cell-matrix interaction. Three-dimensional (3D) *in vitro* tumor models are developed to mimic the complexity and heterogeneity of tumors (Zanoni et al., 2016). In 3D models, the complexity of tumor tissue is mimicked with cell and extracellular matrix interactions (Mohammad-Hadi, MacRobert, Loizidou, & Yaghini, 2018). Some *in vivo* responses such as drug penetration, resistance, hypoxia and deposition in ECM can be better studied and understood in 3D tumor models (Zanoni et al., 2016). As used in many types of

cancers, 3D tumor models have shown reliable results in colorectal cancers as well (Khot et al., 2018). 3D models are commonly used in PDT to study mainly the photosensitizer uptake and the light penetration (Evans, 2015). Also, by using tumor cells as well as healthy cells, 3D tumoroids may be created as an *in vitro* model mimicking the real tumor mass and its environment as much as possible (Zanoni et al., 2016). However, in this thesis work only 3D models comprised of colorectal tumor cells were used.

In this chapter, the detectable PpIX accumulation for a colorectal cancer cell (HCT116 cells) was studied with a wide range of ALA concentrations. The dose dependent dark cytotoxicity and phototoxicity of ALA was determined in 2D cell culture using both Alamar Blue (AB) assay and MTT assay. The reactive oxygen species (ROS) resulting from the PDT was detected at the significant concentrations of PpIX accumulation. Then, 3D early and late cell cultures were developed and the dose dependent cytotoxicity as well as dose-time dependent phototoxicity were determined in 3D models using Alamar Blue, live/dead assays, Annexin V/PI assays. Finally, the interaction of 5FU and ALA was studied in 2D cell cultures to find the best molar ratio for effective PDT-chemo combination.

1.3 Experimental method

1.3.1 Materials

5-aminolevulinic acid (ALA), hydrogen peroxide (H_2O_2) and 2',7'-Dichlorofluorescin diacetate (DCF-DA) were obtained from Sigma (Missouri, U.S.). All chemicals were used at the highest purity.

McCoy's 5A medium, phosphate-buffered saline (PBS) solution and Thiazolyl Blue Tetrazolium Bromide (MTT) were obtained from Sigma (Missouri, U.S.). Fetal bovine serum (FBS), penicillin/streptomycin (pen/strep) solution, trypsin-EDTA solution, 10X Minimum Essential Medium (MEM) and HEPES buffer solution were obtained from Gibco-ThermoFisher (Massachusetts, U.S.). Alamar Blue (AB) viability test and AlexaFluor® 488 (Phalloidin) dye were purchased from Invitrogen (California, U.S.). HCT116 – human colon cancer cells were obtained from ATCC (Virginia, U.S.).

For 3D cell culture study, the RAFT kit was purchased from Lonza (Basel, Switzerland) and rat tail collagen (type I) was obtained from First Link Ltd (UK). LIVE/DEAD Viability/Cytotoxicity kit was obtained from Invitrogen - L3224 (California, U.S.). Annexin V-FITC Apoptosis Detection Kit was purchased from

ABCAM - ab14085 (Cambridge, UK). For cell staining study in 3D cell culture, DAPI dye was obtained in mounting medium, VECTOR (California, U.S.).

1.3.2 Instruments

The photodynamic therapy (PDT) was conducted with the 420 nm LumiSource lamp (PCI Biotech, Oslo, Norway) at UCL. The PpIX fluorescence and viability results were recorded by using the TECAN-Infinite-M200 PRO microplate reader (Switzerland). The results were analyzed by using GraphPad Prism 8 software (California, U.S.). The fluorescence images of cells treated with live/dead viability assay kit and apoptosis detection kit were obtained using EVOS-Life fluorescence microscope equipped with GFP and Texas Red filters (Thermo Fisher Technologies, Massachusetts, U.S.). The phalloidin/DAPI staining of the 3D cell cultures were observed under the Olympus Fluorescence Microscope by using FITC and DAPI filters (Tokyo, Japan).

1.3.3 3D cell study

HCT116 cells were cultured in McCoy 5A complete medium, supplemented with 10% (v/v) FBS and 1% (v/v) pen-strep. Cells were cultured in a 5% CO_2-humidified incubator at 37 °C and were passaged every 2-3 days.

3D cell structures were produced by using the protocol of the RAFT-3D cell culture kit (Lonza, Slough, UK). 1M HEPES buffer solution, 10M NaOH for neutralization, 10X MEM as pH indicator and rat tail collagen (type I) were mixed with the cells. The mixture was separated to 96-well plate as 240 µl/well. After 15 minutes of incubation at 37°C, the RAFT absorbers were placed on the structures. After the structures were pressed by the weight of the absorbers, the absorbers were removed. The cells in the collagen structure were left in the fresh complete medium for 1 day for the early model and 6 days for the late model.

1.3.4 Cytotoxicity assays

For the cytotoxicity assays, the cells were seeded at a density of $7.5x10^3$ cells/well for 2D and $50x10^3$ cells/well for 3D model in 100 µl complete medium into 96-well plates and incubated at 37 °C in 5% CO_2-humidified atmosphere. Cells were incubated until the adequate confluency. Then, cells were washed with PBS, and ALA in different concentrations was introduced to growing cells in serum-free medium. After 48 hours, the cell viability was assessed using both MTT (25 µl 5 mg/ml solution with 75 µl fresh

medium) and Alamar Blue (AB) (10% v/v) colorimetric assay in 2D cell cultures. AB assay was used in 3D models. In the MTT assay, the produced purple formazan crystals are the result of the mitochondrial activity in the viable cells. The absorbance of each sample at 570 nm was recorded using a microplate reader. In AB assay, resazurin reacts with all mitochondrial molecules including cytochromes, which is not reacting with MTT (Rampersad, 2012). The samples were excited at 540 nm and the fluorescence of samples was measured at 570 nm by using a microplate reader.

Cells that were not exposed to ALA were used as controls. 100% viability is assumed for the control cells. The absorbance intensity of the ALA-treated cells without viability assays was determined to eliminate ALA-dependent absorbance in the viability assays reading. The relative cell viability was calculated using the following equation.

$$\%\text{Cell viability} = \frac{\text{Absorbance of sample}}{\text{Absorbance of control}} \times 100$$

1.3.5 PpIX fluorescence detection

The PpIX fluorescence of the samples was recorded by using a microplate reader. The cells were incubated with different ALA concentrations. After 24 hours, cells were washed with PBS and left in PBS during the recording of the fluorescence intensity. Cells were excited at 420 nm and the fluorescence was recorded from 600 nm to 750 nm in 3D cell studies. In 2D cell study, cells were excited at 420 nm and the emission was recorded at 635 nm.

1.3.6 Photodynamic therapy (PDT) experiments

For PDT, cells were incubated with the different concentrations of ALA for 24 hours at 37°C in the 5% CO_2 incubator. Then, cells were carefully washed with PBS and left in fresh complete medium. Except for dark control cells, all plates were irradiated with 7 mW/cm^2 output 420 nm blue light for 5 or 10 minutes. Irradiation was made from the bottom of the plate. Dark control cells were covered with aluminum foil. After irradiation, cells were incubated for a further 24 hours before application of assays.

1.3.7 Detection of reactive oxygen species (ROS)

Reactive oxygen species were detected by using ROS-sensitive DCF-DA dye. DCF-DA dye oxidizes with ROS and turns into a fluorescent molecule, DCF. For this detection, cells were incubated with 600 µM H_2O_2 solution for 30 minutes. Then, the dye solution

was applied to the cells and incubated by covering an aluminum foil in the 37°C incubator for 30 minutes. After incubation, the fluorescence intensity was recorded at 538 nm by exciting at 485 nm with a microplate reader.

1.3.8 Cell staining study

The evaluation of the 3D structures was made with phalloidin and DAPI staining. At the end of the incubations, 3D structures were fixed with 4% formalin for 30 minutes. Then, cells were washed and permeabilized with a mixture of BSA (1% w/v in PBS) and Triton-X (0.3% v/v in PBS) solution. After waiting for 1 hour for permeabilization, cells were washed with PBS and 100 µl 5 µg/ml phalloidin solution was applied to cells for 1-1.5 hour. Cells were washed 3 times with PBS and 3D structures were transferred well to a glass slide with a brush. On the phalloidin stained structures, one drop of nuclear dye DAPI in the mounting medium was also applied. Cells were carefully covered with cover glass and sealed with nail polish. Cells were visualized under the Olympus Fluorescence Microscope with FITC for phalloidin ($\lambda_{Ex/Em}$ 495/518 nm) and DAPI ($\lambda_{Ex/Em}$ 352/461 nm) filters. The structures were stored in dark at 4°C.

1.3.9 Live/Dead assay

For the live/dead assay, incubated cells were stained with calcein AM for live cells and ethidium bromide homodimer (EthD) for dead cells. The kit was applied by using the manufacturer's instructions. After the staining of 3D late models, cells were visualized under the EVOS-Life fluorescence microscope. The stained structures were stored in the dark.

1.3.10 Apoptosis-Necrosis assay

To study the cell death mechanism, the Annexin V-FITC apoptosis kit from ABCAM company was used. Cells were incubated with the FITC labeled Annexin-V and propidium iodide (PI) as the manufacturer's suggestion after the incubations. Annexin V has a high affinity to phosphotidylserine molecules which is translocated from inner face to the cell surface in apoptotic cells. PI binds to double-stranded DNA when the membrane integrity of cells is lost which is the result of necrotic cell death and stains the cells to red fluorescence. 3D early cell structures were observed under the EVOS-Life fluorescence microscope by using a GFP filter for Annexin-V and Texas Red filter for PI.

1.3.11 Statistical analysis

The comparison between more than two results were conducted by using an ordinary one-way ANOVA analysis of variance followed by multiple Dunnett's comparison test of GraphPad Prism 8 software. The significance between the two data was conducted by using the non-parametric Mann-Whitney test of GraphPad Prism 8 software. All results were two-tailed. All measurements were expressed as mean values ± standard deviation (SD). $p < 0.05$ was accepted as a statistically significant difference. All 2D and 3D cell culture experiments were repeated five-times and four-times, respectively.

1.4 Results & Discussions

1.4.1 In vitro ALA-based PDT of HCT116 cells in 2D and 3D cell cultures

The selection of viability assays is vital for correct evaluation of the materials. MTT and AB assays are both popular assays that measure the mitochondrial activity to assess the viability. In general, AB is considered more sensitive when small differences in viability is suspected, however more expensive than the MTT assay (Bonnier et al., 2015; Frame et al., 2016; Hamid, Rotshteyn, Rabadi, Parikh, & Bullock, 2004; O'Brien, Wilson, Orton, & Pognan, 2000). In this study, the 2D cell study was performed with both AB and MTT assays (Figure 1.6). In the MTT assay, the formazan crystals, which are non-soluble in water, were formed by the metabolically active cells and they should be dissolved in DMSO which is appropriate in 2D cell cultures, but not in 3D structures. Therefore, AB is preferred for 3D. In order to be able to compare the viability of cells in 2D and 3D, the use of the same assay is preferred. MTT–AB comparison in 2D was also performed to compare their sensitivity and suitability in studying ALA based toxicity in colorectal cancer cells.

2D-HCT116 colorectal cancer cells were treated with ALA between 0.25 – 1000 µM concentrations. Dark toxicity was determined by MTT and AB after 48h and light toxicity was determined 24h after 5 min irradiation at 420 nm following the initial 24h incubation (Figure 1.6). MTT indicates lower viability in general, but both assays show the difference between dark and light toxicity efficiently. AB, in general, provided more consistent results than MTT assay The IC50 concentration of ALA in the PDT study was determined between 400-600 µM by both assays.

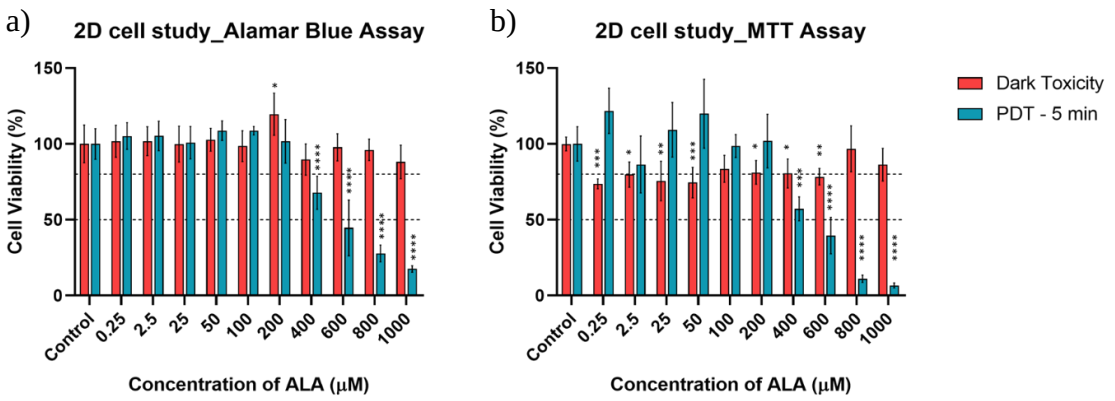

Figure 1.6. The dark and light cytotoxicity (PDT) of ALA in HCT116 cells determined after 48 hours incubations and 24 hours after irradiation at 420 nm. a) Alamar Blue Assay, b) MTT assay. Data were presented as mean ± SD of independent experiments (n = 5). $p < 0.0332$ (*), $p < 0.0021$ (**), $p < 0.0002$ (***), and $p < 0.0001$(****). Dashed lines show the 80% and 50% viability.

For effective photodynamic therapy, the concentration of PpIX accumulated in the cells is essential. The ability of different cells to convert ALA to PpIX show significant differences due to the controlled mechanism of pathways (Eskiler et al., 2020; Krieg et al., 2002; Wawrzyniec et al., 2015). To determine the intercellular PpIX concentrations in the HCT116 cells after 48h incubation, the fluorescence of PpIX was measured in HCT116 cells treated with ALA in the range of 0.25-1000 µM (Figure 1.7). Only at and above 200 µM ALA, the PpIX concentration became detectable via microreader. Also, 800 µM ALA seems to be the maximum amount that may be used since the PpIX amount decreased beyond this concentration in HCT116 cells. In most of the studies, 1mM ALA use in common (Eskiler et al., 2020; Hatakeyama et al., 2013) and some studies no PpIX was detected lower concentrations in glioma cells (Blake & Curnow, 2010).

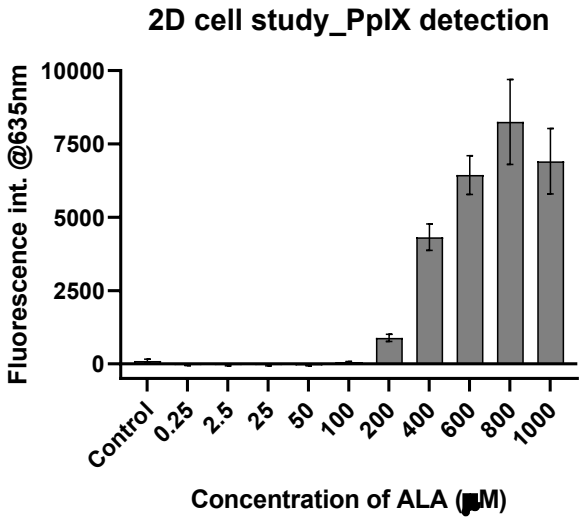

Figure 1.7. The detection of PpIX fluorescence at 24 hours in 2D cell study by excitation at 420 nm.

In PDT, irradiation of PpIX causes the formation of reactive oxygen species (ROS) in the cell. Therefore, ROS levels of 5- and 10-min irradiated cells were determined (Figure 1.8). No significant dependence of ROS level to irradiation time was observed. Significant increase in ROS levels were observed at and above 200 µM ALA in correlation with the significant PpIX generation at and above this concentration. Therefore, it was concluded that for significant ROS concentration, there is a need for a significant PpIX accumulation in the cells and in 2D experiments, this may be achieved with minimum 200 µM ALA and with 5 min irradiation at 420 nm.

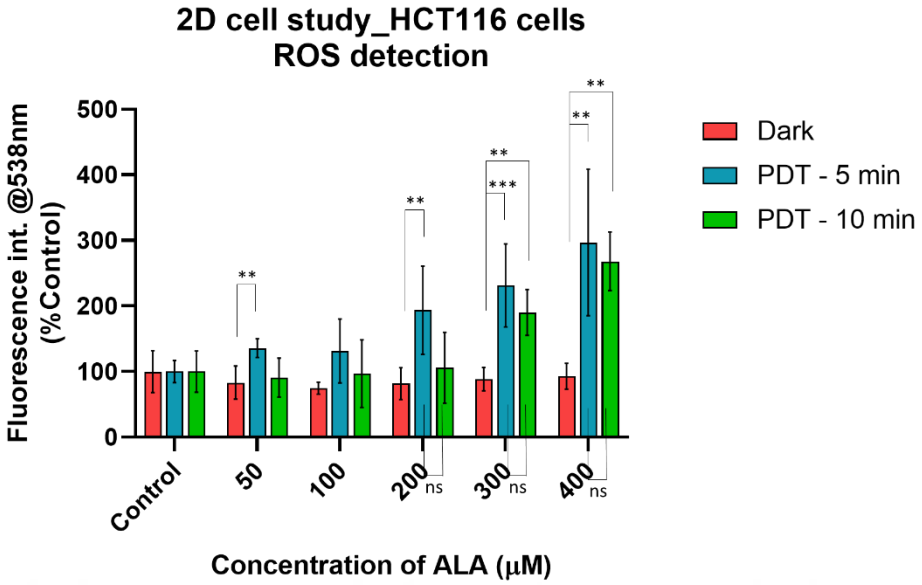

Figure 1.8. Detection of fluorescence of ROS-sensitive DCF-DA dye in 2D HCT116 cell culture. Excitation wavelength: 485 nm, detection wavelength: 538 nm. Data were presented as mean ± SD of independent experiments (n = 4). $p < 0.0332$ (*), $p < 0.0021$ (**), and $p < 0.0002$ (***). n.s.: not significant. Control: untreated cells. Dark: ALA treated but not irradiated cells.

This study was repeated in 3D cell cultures between 100-400 µM ALA concentration, based on the results obtained in 2D. The PpIX fluorescence was recorded between 600-750 nm with 420 nm excitation (Figure 1.9). About 20 times higher PpIX fluorescence than early model was detected in the late model. This enhancement resulted in detectable PpIX amounts even with 100 µM ALA especially in the late model. Comparison of the PpIX emission intensity at 630 nm detected from early and late 3D models show a significant difference in favor of the late model, which is a more populated model. This difference is also reflected in the PDT efficiency. When these early and late models were irradiated for 5-10 min, early model showed a significant reduction in viability of cells at and above 300 µM ALA but in late model toxicity started at 100 µM ALA (Figure 1.10).

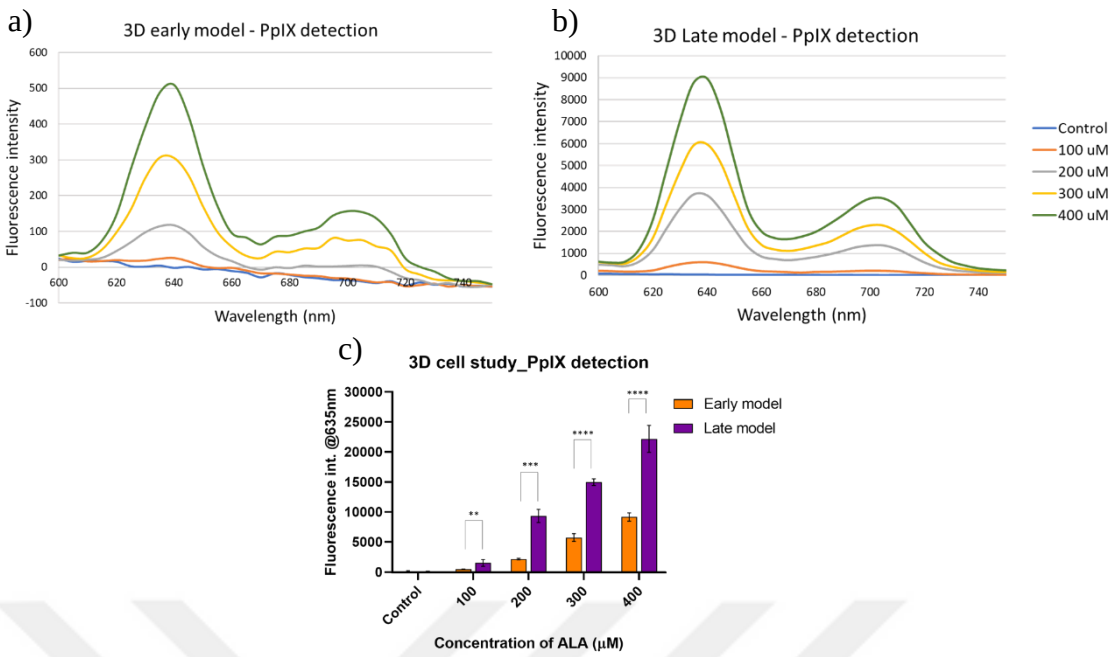

Figure 1.9. Fluorescence spectrum of intracellular PpIX after 24 hours incubation of ALA in 3D-HCT116 a) early model and b) late model. Excitation at 420 nm. c) Comparison of PpIX fluorescence at 635 nm in early and late model. Data were presented as mean ± SD of independent experiments (n = 4). $p < 0.0021$ (**), $p < 0.0002$ (***), and $p < 0.0001$(****).

By the increase in the complexity of the 3D structures, the therapeutic ALA concentration was decreased from 300 µM ALA to 100 µM ALA due to a higher concentration of PpIX accumulation. At highest concentrations in the late model, the irradiation time did not make a dramatic difference due to the complete depletion of the tumor cells; the viability was 12% and 7% in 5- and 10-minutes irradiation, respectively. In the early model and at low concentrations of late model, irradiation time seem to be more important. In early model, with 400 µM ALA, the viability of cells after 5-minutes irradiation was 2.7 times more than 10-minutes irradiation. Overall, late 3D model of HCT116 cells indicates that near 50% cell death by PDT may be achieved by only 100 µM ALA and with 10 min irradiation.

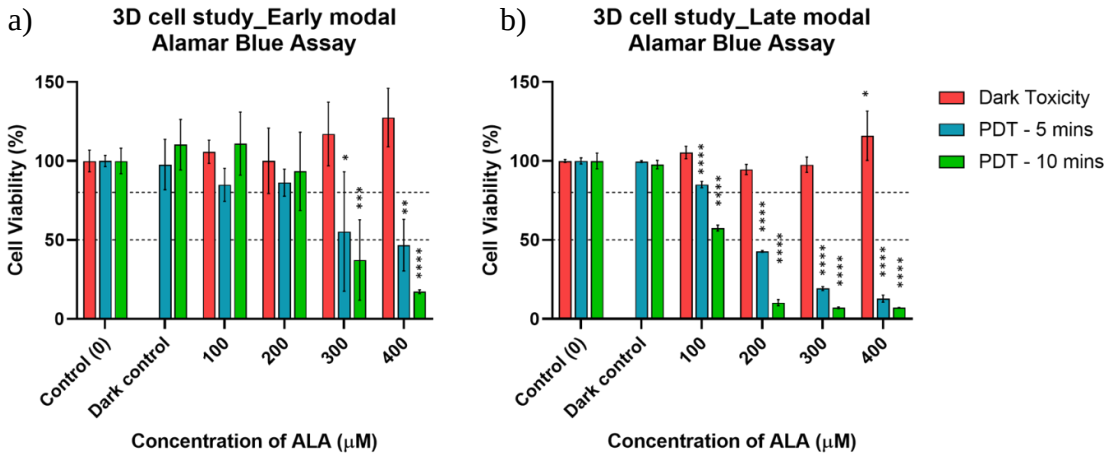

Figure 1.10. The viability (Alamar Blue) assay in 3D a) early and b) late models. Cells were irradiated with 420 nm blue light after 24 hours. Dark toxicity cells were incubated for 48 hours. Data were presented as mean ± SD of independent experiments (n = 5). $p < 0.0332$ (*), $p < 0.0021$ (**), $p < 0.0002$ (***), and $p < 0.0001$(****). Dashed lines show the 80% and 50% viability.

In order to visualize the effect of PDT on cells of the 3D structures, both early and late models were treated with 100-300 µM ALA and irradiated for 5-10 min at 420 nm then stained with DAPI and Phalloidin dyes (Figure 1.11). Destruction of the unity of the clusters in the 3D model was observed as a result of the PDT with supports light toxicity. As seen from the Phalloidin stained cytosols, the cells were burst at high concentrations of ALA. The nucleus of the 3D clusters was still together in both early and late models. Without illumination and /or ALA, dark control cells (Not irradiated and not treated ALA), dark (Not irradiated but treated with ALA) and control (Not treated with ALA but irradiated) cells were showed bright and perfectly clustered images.

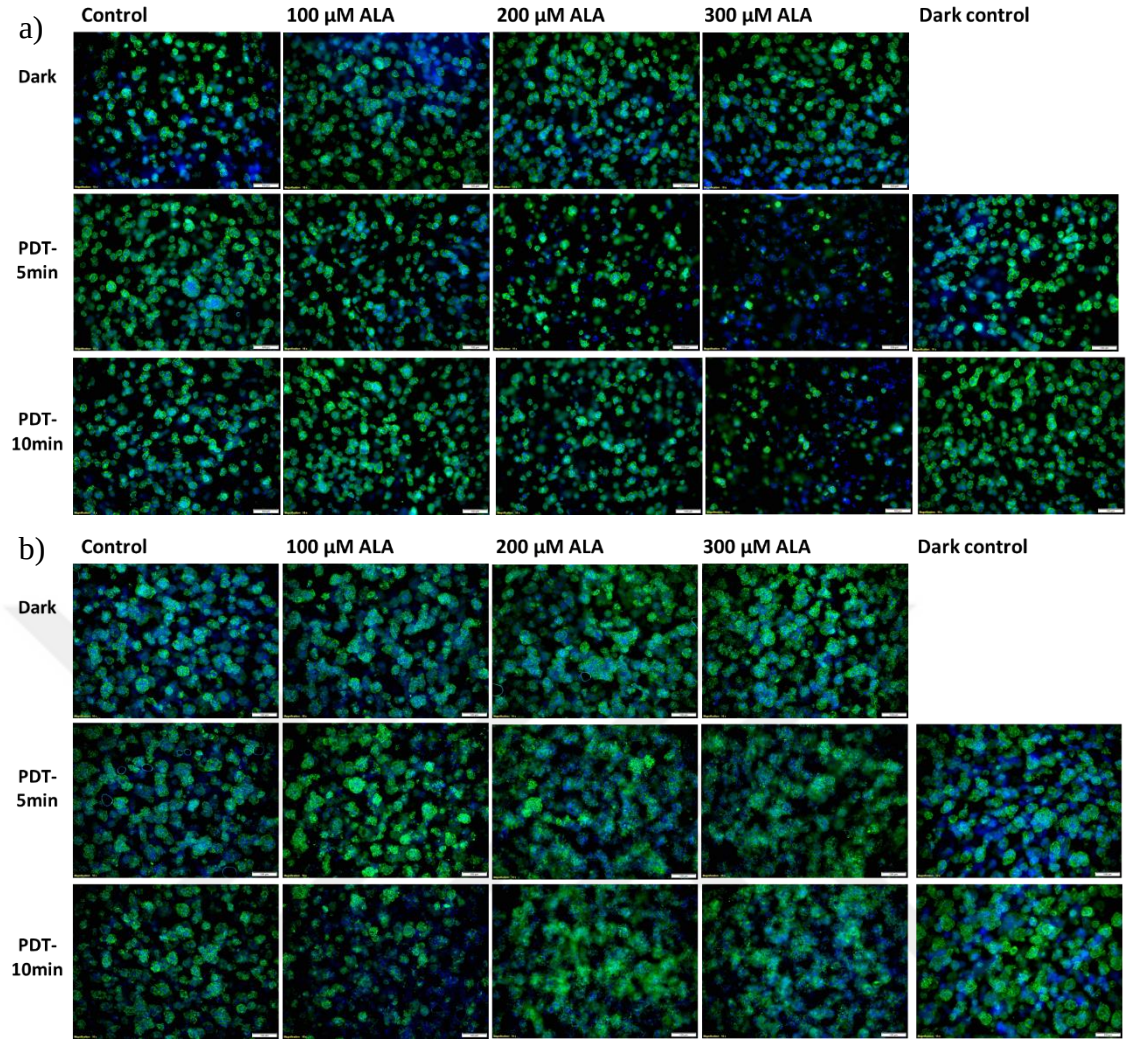

Figure 1.11. Phalloidin/DAPI staining of 3D a) early and b) late models. Dark: ALA treated but not irradiated cells, Dark control: Not irradiated control cells, Control: Irradiated control cells. Magnification:10X. Scale bar: 100 µm.

To correlate the reduction in viability measured as a function of mitochondrial activity of live cells, to the cell death, live/dead assay was performed on late 3D cellular structures treated with ALA between 100-400 µM concentration and irradiated at 420 nm for 5-10 min (Figure 1.12). Calcein AM used in the staining turns into a green fluorescent calcein by the esterase activity of the live cells and propidium iodide penetrates into the cells only when the cellular membrane integrity is lost and causes a strong red fluorescence when binds to nucleic acids. Therefore, green fluorescence indicates live cells are red fluorescence indicates dead cells. Strong green fluorescence was observed in control cells (lack ALA but irradiated) and dark control cells (lack ALA and irradiation) indicating no cell death due to only irradiation or ALA treatment. After illumination, the green fluorescence did not change significantly at low ALA concentrations. However,

especially in high concentrations, the red fluorescence from dead cells was observed clearly, even in the center of the 3D clusters. The observation of the dead cells at the center in both the early and late models is an important indication of the PDT and promising for *in vivo* treatment of solid tumor.

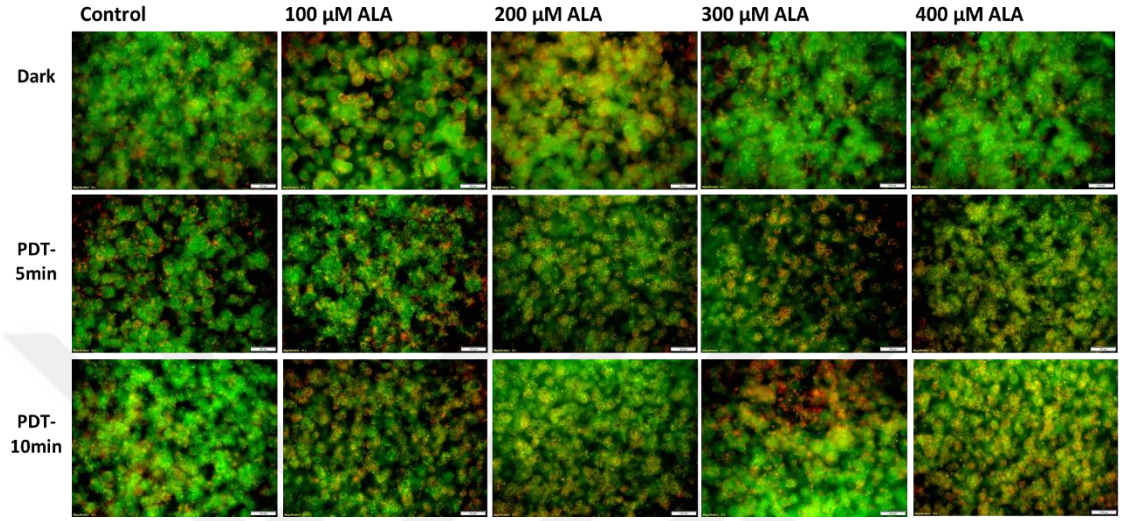

Figure 1.12. Live/dead staining of 3D late model. Green: Calcein-Live cells, Red: Ethidium bromide homodimer -Dead cells. Dark: ALA treated but not irradiated cells, Control: Irradiated control cells. Magnification: 10X, Scale bar: 100 µm.

Mode of cellular death was analyzed by Annexin V-FITC Apoptosis Staining Kit in 3D early model using fluorescent microscopy at only 200 µM ALA concentration (Figure 1.13). Both Annexin V and PI negative cells are considered as healthy cells or non-apoptotic/necrotic cell death in general. However, the green fluorescence (Annexin V-FITC), which is usually described as early apoptotic cells, was observed in control and dark cells, as well. This is in contrast to viability assay (Figure 1.10). The high cell density and the skipped washing step–after applying the assay could be the reason of the background green fluorescence. The red fluorescence (PI), described as necrotic cell death, was increased significantly with ALA administration and 10 min irradiation time. Few red fluorescence in the control cells may be due to the nonspecific staining. The observed cell death could not be determined with the cytotoxicity assay in 3D early model.

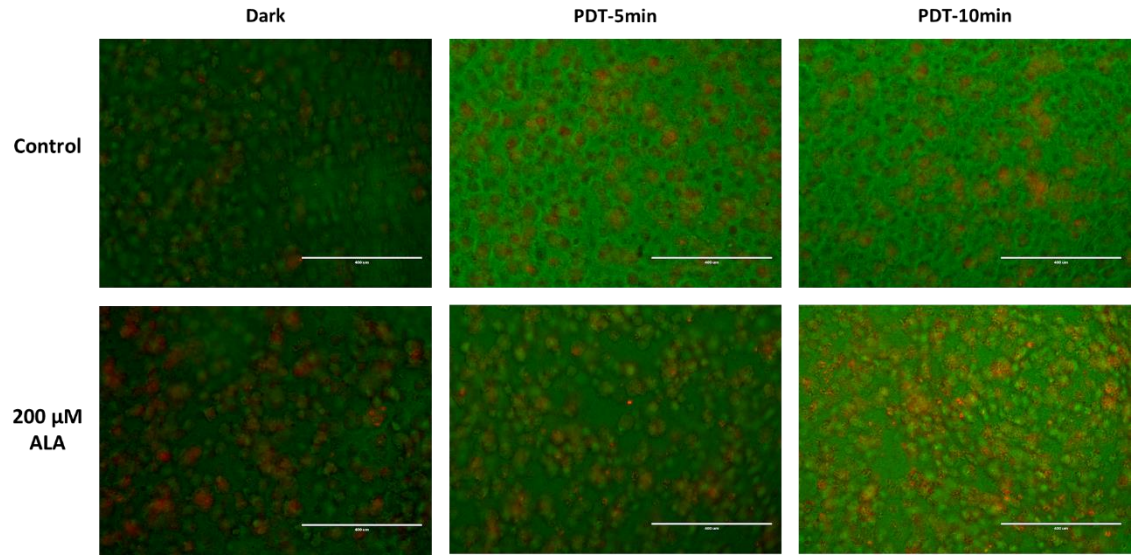

Figure 1.13. Annexin V-FITC / Propidium iodide (PI) assay in 3D early model. Green: Annexin V – Early apoptotic cells. Red: PI – Necrotic cells. Control: Not irradiated but treated with ALA. Magnification: 10X, Scale bar: 400 µm.

1.4.2 Investigation of 5FU and ALA interaction for combination therapy

The main goal of project # 216Z131 funded by TUBITAK and British Council is the treatment of colorectal cancer via targeted combination therapy. This involves combination of ALA-based PDT with 5FU. There are a few encouraging articles showing higher cytotoxicity due to accumulation of higher concentration of ROS when ALA and 5FU combination was used in a sequential manner or simultaneously (Benito-Miguel, Blanco, & Gomez, 2015; Tahmasebi, Khoshgard, Sazgarnia, Mostafaie, & Eivazi, 2016).

Here, HT-29 colorectal cancer cells were treated with ALA and 5FU combination simultaneously at different mol ratios and PpIX level of the treated cells were measured. PpIX levels of cells treated with ALA (32-512 µM), 5FU (36.2-587.2 µM) and the combination were determined 48 h after incubation. 5FU dose range is selected for different levels of toxicity. As expected, 5FU did not produce any PpIX. ALA to PpIX conversion was observed in the whole concentration range and PpIX accumulation increased with the ALA concentration as expected with kind of saturation around 256 µM. At 1/1.15 ALA/5FU mol ratio, when cells were co-incubated with the two agents, a significant reduction in the PpIX production was observed (Figure 1.14a). However, when ALA excess combination is used, 1/0.15 ALA/5FU, PpIX production at similar amounts to free ALA was observed (Figure 1.14b) between 150/23 µM ALA/5FU-

512/76.6 µM ALA/5FU formulations which are sufficient for PDT and chemotherapy effect, individually. The role of 5FU in ALA-based PpIX production, which is clearly an inhibition, is not known, but we suggest that the cyclic PpIX formation from ALA involves nucleophilic attach of amine to carbonyl of the ALA, and amine/carbonyl groups of 5FU may hinder this process. Combination of 5FU and ALA via tumor targeting nanoparticles will be reported in the doctoral thesis of Mahshid Hashemkhani (KU).

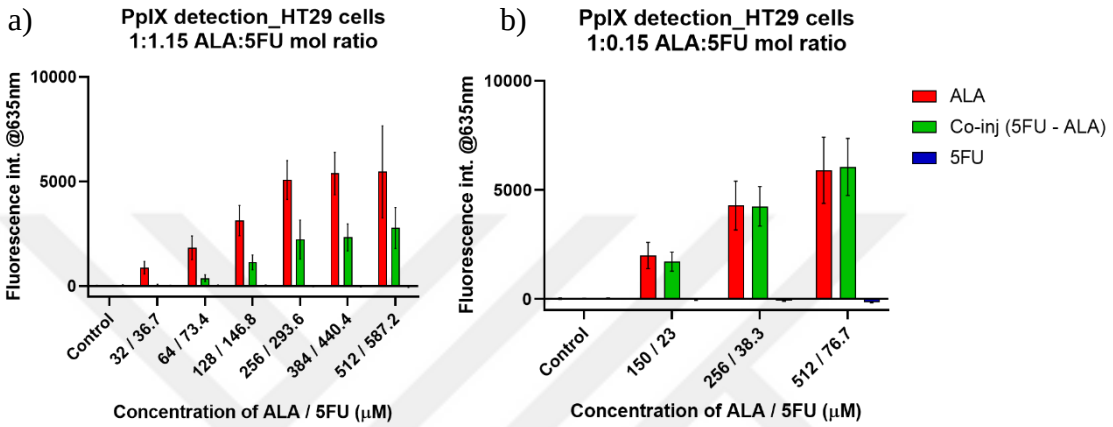

Figure 1.14. The detection of PpIX fluorescence at 24 hours in HT-29 cells by co-injection in (a) 1: 1.15 and (b) 1:0.15 ALA: 5FU mol ratio.

1.5 Conclusion

PDT is a promising local, mild therapeutic approach in cancer treatment. ALA-based PDT is quite popular, especially after the recent FDA approval. Response of different cells, hence tumors, to PDT show differences, since ALA-PpIX conversion show differences between different tumor cells. Effective ALA concentration and irradiation time needs to be optimized for effective PDT for the studied tumor type. Here, ALA to PpIX conversion in a broad ALA concentration was studied on HCT116 colorectal cancer cell lines both in 2D and 3D tumor models. Dose adjustment was initially performed in 2D and hence tests were performed in a narrower concentration range in early and late 3D models. Development and application of experiments in 3D is vital before translation of the knowledge to animal studies since 3D models represent the complexity of real solid tumors better. Hence, 100 µM ALA and 10 min irradiation was confirmed as a good protocol for further ALA-based PDT of the colorectal tumors, at least *in vitro*. Light toxicity was related to ROS and consequent apoptosis/necrosis of the tumor cells in 2D and 3D cell cultures.

In addition, for possible combination of ALA-PDT with classic 5FU chemotherapy in the treatment of colorectal cancer, co-injection of the two was studied in another colorectal cancer cell line (HT-29). An apparent interference of 5FU with ALA-to-PpIX conversion was detected, hence, molar excess of 5FU reduces the PpIX accumulation dramatically which would limit PDT efficiency, however, at still acceptable doses of 5FU if ALA excess combination is used, high PpIX levels can be obtained for effective combination therapy.

In further combination therapies, either sequential addition of the two or the optimized 1/0.15 mol ratio of ALA/5FU should be considered. In the continuation of this project, we have loaded the two agents to a nanoparticle with different routes to ensure release at different times in addition to the optimized ratio of the two. To follow up, readers are recommended to read the PhD thesis of Mahshid Hashemkhani.

1.6 Acknowledgement

The study was a part of a collaboration between Koç University (KU) and University College London (UCL) funded by TUBITAK (grand number 216Z131) and British Council. I would like to thank the UCL supervisors Prof. Dr. Alexander J. MacRobert, Prof. Dr. Marilena Loizidou and the collabator Dr. Layla Mohammad-Hadi for their guidance and contributions. All 2D-and 3D- PDT studies presented here were performed in UCL laboratories by Gozde Demirci. I would like to also acknowledge Mahshid Hashemkhani who is the PhD student working on adaptation of the knowledge gained here to nanoparticles for the completion of the project.

Chapter 2: Delivery of Genes by Novel Polymers

Introduction

Osteosarcoma (OS) is an aggressive cancer type that has been affecting children and adolescents (Sayles et al., 2019; Tan, Choong, & Dass, 2009). Unfortunately, the treatment regimens did not change dramatically for the last 30 years. Combination of multiagent chemotherapy and surgery is the primary approach in the clinic. However, a significant portion of the patients are resistant to chemotherapy, and severe side effects of chemotherapy limit the recovery and survival (Sayles et al., 2019; Tan et al., 2009). Recent efforts directed towards overcoming these limitations and finding alternative therapeutic methods focus on gene therapy, which became possible after the recent genetic profiling of the osteosarcoma (Subbiah et al., 2015). However, designing an effective and safe gene delivery vehicle to carry the therapeutic genetic material into bone tissues remains a challenge (Sayles et al., 2019)

2.1 Gene Delivery Vesicles

Gene therapies are becoming a prevalent solution for silencing/replacing gene abnormalities in genetic diseases and for altering the expression of genes in cancerous cells (Martinez-Negro et al., 2019; Pack, Hoffman, Pun, & Stayton, 2005), and gene delivery systems have already been tested in the treatment of various cancers (Kean, Roth, & Thanou, 2005; Pack et al., 2005; Wan, Qian, Li, & Li, 2015). The biggest challenge in gene therapy is the safety of the transfection vesicle and efficiency of the vesicle to transfer the gene (Almulathanon, Ranucci, Ferruti, Garnett, & Bosquillon, 2018). Viral vectors have shown high transfection efficiency to various areas of the body (Choi, Kang, Kim, Lim, & Chung, 2010; Ohashi et al., 2001). Due to possible immunogenetic and sterilization problems of viral vectors, the safety becomes an issue and therefore, viral vectors are not preferred for gene delivery in the clinic (Almulathanon et al., 2018; Kean et al., 2005; Lin & Engbersen, 2008; Pack et al., 2005). Non-viral gene-carrier systems have become a good alternative in transfection studies due to considerable safety improvement despite their lower efficiency (Choi et al., 2010).

Non-viral gene-delivery systems based on cationic entities including dendrimers (Kumar, Yellepeddi, Davies, Strychar, & Palakurthi, 2010; Zinselmeyer, Mackay, Schatzlein, & Uchegbu, 2002), polymers (Lin & Engbersen, 2008; Piest & Engbersen, 2010) and lipids (Digiacomo et al., 2018; Martinez-Negro et al., 2019) have drawn the

attention of scientists due to their simple electrostatic interaction between positively charged functional-groups and the negatively charged phosphate groups on nucleotides (Braun et al., 2005). Delivering the genetic material with such cationic vesicles decreases the amount of gene degradation that is otherwise caused by nucleases and improves the transportation efficiency through the cell membrane by endocytosis/phagocytosis (Abedi-Gaballu et al., 2018; Kumar et al., 2010). Through functionalization of the vesicle surface with targeting moieties, the efficiency of the therapy may be increased further (Gu, Wu, Chen, & Xiao, 2013; Huang, Ke, Liu, Jiang, & Pei, 2008). Most widely used cationic polymers are poly(ethyleneimine) (PEI) and poly(L-lysine). However, some critical challenges still exist for these cationic polymers that need to be overcome to be translated to the clinic. One of the setbacks is the tradeoff between the transfection efficiency and cytotoxicity of the polymers. Increasing the molecular weight of the polymer increases the loading efficiency of DNA, but it increases the toxicity (Almulathanon et al., 2018; Zinselmeyer et al., 2002). Hence, PEI 25 kDa is considered as the gold standard with an acceptable balance of these issues. Various structural modifications were made to increase the biocompatibility of the cationic polymers. One common strategy is the integration of polyethylene glycol (PEG) as a biocompatible component (Almulathanon et al., 2018; Kim et al., 2004). Another one is the replacement of primary amines with alcohol functionality (Lee et al., 2003). These modifications increase the biocompatibility *in vivo*, mostly by reducing the charge density yet decrease the loading efficiency of the genetic material, the internalization of the resultant complexes and/or the endosomal release of the plasmid (Almulathanon et al., 2018; Lee et al., 2003). Cationic polyplexes enter cells via endocytosis and they have to escape from the endosome into the cytoplasm before fusing with lysosomes, which is called as endosomal escape. This was attributed to the protonation of amines in the acidic microenvironment which causes osmotic swelling and membrane rapture which is known as the proton sponge effect or to the formation of transient pores on the endosomal membrane releasing the cargo into the cytoplasm, which is proposed as an alternative mechanism for endosomal escape of polyplexes (Godbey, Kenneth, & Mikos, 1999). The genetic cargo is released near or inside the nucleus (Lin & Engbersen, 2008). However, cationic polymers may also damage plasma, nuclear and/or mitochondrial membrane and trigger apoptotic/necrotic events resulting in significant toxicity (Almulathanon et al., 2018; Choi et al., 2010; Moghimi et al., 2005). Non-degradable backbone of PEI may also contribute to the long-term toxicity (Choi et al., 2010; Godbey et al., 1999).

Degradable polymers with amine functionalities and lower charge density are considered as alternative vehicles for gene delivery. Poly(amidoamine) s (PAAs) with peptide-mimicking backbones are a class of synthetic, biodegradable and relatively less-toxic polymers investigated for gene delivery. Poly(amidoamine)s (PAAs) with peptide-mimicking backbones are a class of synthetic, biodegradable and relatively less-toxic polymers despite their cationic character; and considered to have great potential for biomedical applications, including drug, protein, and gene delivery (P. Ferruti, Marchisio, & Duncan, 2002; Y. Sun et al., 2017). They have *tert*-amine groups at their backbone and synthesized by stepwise polyaddition of primary or secondary amines to bisacrylamides (in solvents such as water or alcohols, at temperatures about 10 °C or above, without catalysts (Manfredi, Ranucci, Suardi, & Ferruti, 2016)), a method that also allows the incorporation of various functionalities to the structure of the polymer (Choi et al., 2010; Piest & Engbersen, 2010).

Primary or secondary amine groups have been added to PAAs to increase their transfection efficiency, which is limited due to the steric effect of the tertiary amines. In particular, PAAs with aminobutyl groups in the side chain have shown higher transfection efficiency than branched 25 kDa PEI (L. Peng, Gao, Xue, Huang, & Zhuo, 2010).

2.2 Bone Targeting

The main handicap with delivery systems is that upon systemic administration of the cargo vesicles into the body, they will be transported to all cells in the body and will be internalized by every tissue. This has also been the main challenge in chemotherapy, including the chemotherapeutic treatment for osteosarcoma (Gu et al., 2013). By functionalization of the vesicles with a targeting molecule, the internalization of the therapeutic vesicle by tumor cells can be increased. In the OS treatment, bisphosphonates are used as the targeting molecule.

Bisphosphonates (BP), especially the nitrogen-containing ones, are used clinically to control bone resorption frequently encountered in osteolytic bone metastasis of various cancers including breast, prostate and lung, osteoporosis, Paget`s disease and rheumatoid arthritis (Gu et al., 2013; Lipton, 2008; M. Sun, Iqbal, Singh, Sun, & Zaidi, 2010). BPs bind to mineralized bone tissue due to the high affinity of BPs to Ca^{2+} to internalized by osteoclasts. They inhibit a key enzyme in the mevalonate pathway and disrupt normal cell function (Conry, Rodriguez, & Pressey, 2016; Lipton, 2008). Non-amine-containing

bisphosphonates, the first-generation BPs, initiates apoptosis in osteoclasts by acting as a cytotoxic ATP analogue (La-Beck, Liu, Shmeeda, Shudde, & Gabizon, 2019). The cytotoxic ATP inhibits various enzymes interacting with ATP (La-Beck et al., 2019). The nitrogen-containing BPs, namely alendronate (ALE), risedronate, ibandronate and zoledronic acid are clinically used for prevention and treatment of osteoporosis (M. Sun et al., 2010). In recent years, nitrogen-containing BPs are also recognized for their direct and indirect antitumor activity associated with inhibition of angiogenesis and tumor progression (La-Beck et al., 2019; Lipton, 2008). There are several reports on OS and metastasis inhibition of nitrogen-containing BPs via anti-proliferative and anti-angiogenic activity (Conry et al., 2016; Ohba et al., 2014). The high affinity of BPs for bone is also utilized to target drugs and drug-carrying nano-vesicles to the bone which would enhance the drug efficacy, reduce off-site effects and required effective dose, hence BP functionalized vesicles have been shown to target tumor-induced osteolysis (Gu et al., 2013; Lipton, 2008; Pignatello et al., 2009; M. Sun et al., 2010).

2.3 Research Proposal

Best properties of branched PEI and PAAs can be combined to design bone targeting, biocompatible, biodegradable new polymeric gene delivery vehicles. For this purpose, PAAs containing 5-amino-1-pentanol (AP) which has been shown as an effective component in PAA based gene transfection, and phosphonic acid (APA) or bisphosphonic acid (ALE) as bone targeting moiety is proposed. Then, to enhance the gene binding and release properties, these PAAs were reacted with short chain branched PEI of 1800 Da molecular weight, producing bone targeting PAA-PEI copolymers (PAEI). ALE and APA was introduced by replacing the AP content by 10-30-50% to investigate the influence of these anionic components in the toxicity and transfection efficiency of PAEIs. There are only two reports on combination of PAAs and PEI in the literature, where bioreducable S-S linkages were introduced to polymer backbone and transfection efficiencies similar or better than PEI 25kDa were observed (Deng et al., 2011; Feng et al., 2015). However, they lack any tumor or organ targeting function. This is the first study investigating the cytotoxicity and gene transfection ability of phosphonic acid or bisphosphonic acid functionalized PAEIs for targeting therapeutic genes to bone. As a model, green fluorescence protein (GFP) was studied. Hard to transfect U-2 OS cells and healthy myoblast cells (C2C12 cells) were used for both toxicity and transfection experiments.

All results were compared with 25 kDa bPEI, 1.8 kDa bPEI and FuGENE®, which is a commercial transfection agent successfully transfecting U-2 OS cells.

2.4 Method

2.4.1 Materials

All polymers were provided by Seçkin Altuncu and Melek Naz Güven at at Boğaziçi University under the supervision of Prof. Duygu Avcı Semiz.

Dulbecco's modified Eagles medium (DMEM) with and without phenol red mediums, fetal bovine serum (FBS), penicillin/streptomycin (pen/strep) solution and trypsin-EDTA were obtained from Diagnovum (Ebsdorfergrund, Germany). OPTI-MEM® I (1X) was bought from Gibco, ThermoFisher (Massachusetts, U.S.). Thiazolyl Blue Tetrazolium Bromide (MTT) was purchased from Goldbio (Missouri, U.S.). FuGENE® HD Transfection Reagent was obtained from Promega (Wisconsin, U.S.). pMX-GFP retroviral vector was bought from Cell Biolabs, Inc. (California, U.S.). Plasmid purification kit was obtained from Macherey-Nagel (Düren – Germany). U-2 OS – bone osteosarcoma epithelial cells were a kind gift from Devrim Gozuacik -Sabancı University (Istanbul, Turkey) and C2C12 – mouse myoblast muscle cells were purchased from ATCC (Virginia, U.S.).

2.4.2 Instruments

The characterizations of the polymers were made by Seçkin Altuncu and Melek Naz Güven at Boğaziçi University under the supervision of Prof. Duygu Avcı Semiz.

The cell viability was measured by using Synergy – H1 microplate reader, BioTek Instruments Inc. (Vermont, U.S.). The hydrodynamic size and charge of the polymers and complexes were measured using Malvern Zetasizer Nano ZS, Malvern Instruments (United Kingdom). The concentration of plasmid was measured by NanoDrop2000 – Thermo (U.S.). Transfection efficiency was tracked by visualizing the green fluorescence protein (GFP) signal produced by cells under a Nikon Eclipse TS100 fluorescence microscope (Japan) equipped with a GFP filter. Transfection efficiency was quantified by using a FACSCalibur™ instrument - Becton, Dickinson and Company (U.S.).

2.4.3 Preparation of polymers

The polymers were synthesized by Seçkin Altuncu and Melek Naz Güven at Boğaziçi University. Control polymer (PAEI-C) was obtained by mixing PAA macromers and 1.8

kDa bPEI at molar ratio of 4:1 (PEI to PAA). For the bone targeted gene therapy, the amino phosphonic acid (APA) and alendronate (ALE) was added to the structure in different ratios with respect to 5-amino-1-pentanol (AP) of the macromer. The different PEI/TETA: PAA ratios were studied in phosphonic acid containing polymer compositions. PAEI's (PAEI-1 to PAEI-6) were prepared from the reaction of PAA macromers with PEI at a mol ratio of 1: 4 or 1:2 ratio in PAEI-8. Another PAEI (PAEI-7) was synthesized from the reaction of PAA macromer, containing 0.9:0.1 AP: APA, with TETA at a mol ratio of 1:2 to observe the effect of PEI (Table 2.1, Figure 2.1).

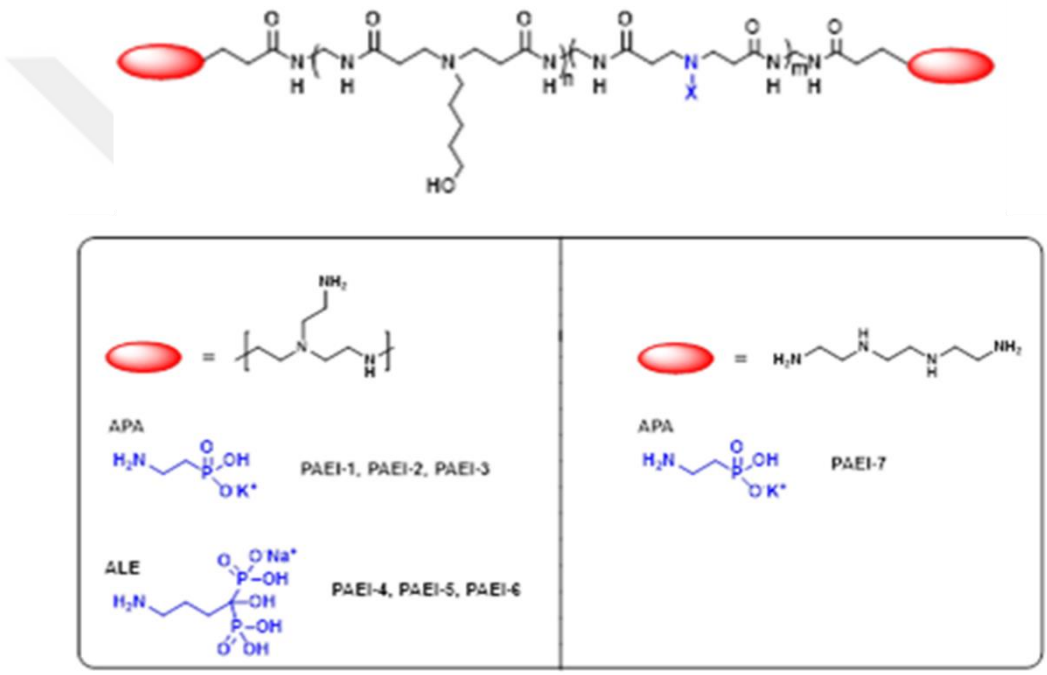

Figure 2.1. Chemical structures for (bis)phosphonic acid functionalized PAEI polymers. APA: 5-Amino phosphonic acid, ALE: Alendronate (a nitrogen containing bisphosphonic acid).

Table 2.1. Mole ratios of functional groups of PAEIs

PAEI	**PEI/TETA: PAA (mol ratio)**	**AP: ALE: APA (mole ratios in feed)**
PAEI-C	4:1	1.0 : 0 : 0
PAEI-1	4:1	0.9 : 0.1 : 0

PAEI-2	4:1	0.7 : 0.3 : 0
PAEI-3	4:1	0.5 : 0.5: 0
PAEI-4	4:1	0.9 : 0 : 0.1
PAEI-5	4:1	0.7 : 0 : 0.3
PAEI-6	4:1	0.5 : 0 : 0.5
PAEI-7	2:1*	0.9 : 0 : 0.1
PAEI-8	2:1	0.9 : 0 : 0.1

*TETA: PAA, TETA: Triethylenetetramine

2.4.4 Cell culture

U-2 OS and C2C12 cells were cultured in DMEM, with and without phenol red complete medium respectively, supplemented with 10% (v/v) FBS and 1% (v/v) pen-strep. Cells were cultured in a 5% CO_2-humidified incubator at 37 °C and were passaged every 2-3 days.

2.4.5 Cytotoxicity assay

For the cytotoxicity assay, the cells were seeded at a density of $1x10^4$ cells/well in the complete medium into 96-well plates and incubated at 37 °C in 5% CO_2-humidified atmosphere until 60-80% confluency. Then, the polymers in different concentrations ranging from 1-100 µg/ml were introduced onto growing cells. After 48 hours, the cell viability was assessed using MTT colorimetric assay by the addition of 50 µl of MTT solution (5 mg/ml in PBS) into each well with 150 µL of culture medium and incubated for 4 h. The purple formazan crystals that were formed because of mitochondrial activity in viable cells were dissolved through the addition of ethanol: DMSO (1:1 v/v) mixture. Each sample's absorbance at 570 nm with a reference reading at 650 nm was recorded using a Synergy – H1 microplate reader. Cells that were not exposed to polymers were used as negative controls. 100 % viability is assumed for the control cells. The relative cell viability was normalized with respect to the control cells, and calculated via the following equation:

$$Cell\ viability\ (\%) = \frac{Absorbance_{sample}}{Absorbance_{control}} \text{x } 100$$

2.4.6 pMX-GFP plasmid

The commercial pMX-GFP (5.3 kb) retroviral vector was propagated in *Escherichia coli* culture and purified by using NucleoBond® Extra Midi Plus - Plasmid Purification Kit (Macherey-Nagel, Düren, Germany) by following the manufacturer's instructions (Wan et al., 2015). The concentration of DNA was determined by measuring the UV absorbance of DNA at 420 nm using a NanoDrop instrument.

2.4.7 Preparation of polyplexes

The commonly used DNA: polymer weight ratio for PAAs was reported as 1:10 in many previous studies (Abedi-Gaballu et al., 2018; Almulathanon et al., 2018; Huang et al., 2008; Kean et al., 2005; Piest & Engbersen, 2010) and also verified in our preliminary studies. For the cell transfection studies, 1 µg polymer and 0.1 µg DNA (GFP plasmid) were mixed in 40 µl OPTI-MEM® and incubated at room temperature for 15-20 minutes. FuGENE® and PEI (branched, 25 kDa) were also used for comparison and as a positive control. For PEI, 1:10 (w/w) ratio was adopted, as well. FuGENE®: DNA ratio was used as 3 µl: 1 µg according to the manufacturer's protocol.

2.4.8 Characterization of polyplexes

Gel retardation assay

Polyplexes were loaded on a 1% agarose gel containing SYBR Green (0.01% v/v) and were subjected to electrophoresis at 100V for 1 h. The plasmid alone was used as a control for the plasmid bands, and band weight was referenced to a 1 kDa DNA ladder.

Hydrodynamic size, zeta potential and polydispersity index measurement

Hydrodynamic size, zeta potential and polydispersity index of the polymers and polyplexes were measured by dynamic light scattering in OPTI-MEM®. All measurements were made with 5 replicas. The plasmid alone was also characterized for comparison.

2.4.9 Transfection studies

Cells were seeded in 96-well plates at a density of $1x10^4$ cells/well and cultured overnight in 200 µl of complete medium to afford 60-80% confluency and were washed once with PBS. Then, 40 µl of the freshly prepared polyplex solution and 160 µl OPTI-MEM® were added to each well. After 12 hours at 37°C, cell medium was replaced with

fresh OPTI-MEM®, and the cells were further incubated for 36 hours to allow gene expression. Overall, transfection efficiency was evaluated 48 hours post-transfection.

2.4.10 Quantification of transfection efficiency

Transfection efficiency of both C2C12 cells and U-2 OS cells was evaluated visually by using a Nikon Eclipse TS100 fluorescence microscope equipped with a GFP filter. Cells that were not exposed to complexes were used as a control. Transfection efficiency in U-2 OS cells was quantified by FACS (Fluorescence-activated cell sorting). Briefly, 1.5 x 10^5 cells/well were seeded into 6-well plates and incubated overnight. Transfection procedures were carried out as described above, and cells were incubated with transfection agents for 48 hours. Then, cells were detached with trypsin and collected into sterile Falcon tubes. Cells were centrifugated and the supernatant was discarded. Precipitated cells suspended in 350 µl PBS and 10^4 cells were read by a BD FACSCalibur™ instrument equipped with a FITC (Fluorescein isothiocyanate) filter and analyzed with the help of CellQuest Pro software.

2.4.11 Statistical analysis

For statistical analysis of the MTT results, one-way ANOVA analysis of variance followed by multiple Dunnett's comparison test of GraphPad Prism 8 software package (GraphPad Software, Inc., USA). Significance between hydrodynamic sizes, zeta potentials and polydispersity indexes (PDI) of polymers and polyplexes was conducted by using the non-parametric Mann-Whitney test of GraphPad Prism 8 software. All results were two-tailed. All measurements were expressed as mean values ± standard deviation (SD). $p < 0.05$ was accepted as a statistically significant difference.

2.5 Results & Discussion

2.5.1 Cytotoxicity of polymers

All polymers were synthesized, purified and characterized by Prof. Avcı's research group at Boğaziçi University.

Cytotoxicity of these polymers were tested between 1-100 µg/ml concentrations on U-2 OS cells (Figure 2.2). Both linear and branched 25 kDa PEIs, which are traditionally used in transfection studies, and 1800 Da bPEI, which was used in the production of PAEIs, were also tested for comparison. High molecular weight PEIs showed significantly high toxicity in U-2 OS cells at 5-10 µg/ml, while low molecular weight

branched PEI (1800 Da bPEI) did not cause any significant reduction in cell viability up to 100 µg/ml polymer concentration (Figure 2.2a). PAEI-C, which was produced as a (bis)phosphonic acid lacking PAA-PEI copolymer caused slightly lower cell viability at high concentrations than 1800 Da bPEI, but significantly better viabilities than both the linear and branched 25 kDa PEI at all doses. Replacement of AP with phosphonic acid (APA) in 10 and 30%, as in the case of PAEI-4 and PAEI-5, decreased the cytotoxicity of the cationic polymers and PAEI-C at the high doses, 50 µg/ml and 100 µg/ml. Cells treated with PAEI-5 showed 60.5% viability at 100 µg/ml, while PAEI-C cased 12% viability at the same dose. This indicates better cytocompatibility of the cationic polymers with APA incorporation and better tolerance at high concentrations. However, when the APA ratio was increased even further (PAEI-6), significant cytotoxicity was observed, especially in high concentrations. This may be due to cytotoxicity of APA at such concentrations and/or due to some conformational changes at 50% incorporation of the phosphonic acid to amine containing copolymer.

PAEI-7 is analogous to PAEI-4 but lacks PEI. It did not show any significant cytotoxicity to U-2 OS cells (Figure 2.2a). Even at the highest polymer concentration, the polymer was well tolerated, and cell viability was around 75%. This result shows that poly(amidoamine)s are biocompatible even at high concentrations (100 µg/ml) tested here (Choi et al., 2010). About 45% difference in viability at 100 µg/ml between PAEI-4 and PAEI-7 originates from the PEI component, most probably due to the increase in positive charge on the polymer. Interestingly, when the PEI ratio was increased, cytotoxicity slightly decreased. For instance, at 50 µg/ml polymer concentration, the viability increased from 55.5 % in 2:1 PEI: PAA (PAEI-8) to 62.5 % in 4:1 PEI: PAA (PAEI-4). This outcome could be a result of better micelle formation and hindrance of the positively charged amine groups. As a result, we continued the studies and modifications with the higher ratio of PEI containing polymers for better transfection properties, since lower PEI amount did not provide a dramatic advantage in toxicity.

Bisphosphonic acid (ALE) containing polymers (PAEI-1,2,3) showed better cytocompatibility than high molecular weight PEIs. Interestingly, PAEI-3 with 0.5-0.5 AP and ALE showed significant cytotoxicity only at 100 µg/ml with viability higher than the value observed with 1800 Da bPEI and PAEI-C. When the amount of ALE was decreased (PAEI-1 – 10% and PAEI-2 – 30%), the viability was decreased more than three times. For instance, at 100 µg/ml, PAEI-3 showed 37.5% viability while PAEI-1

and 2 showed around 10% viability. This may be related to different conformational structures of the copolymer with different anion/cation ratio.

As known from the literature, alendronate accelerates bone regeneration by binding to the hydroxyapatite (Kennel & Drake, 2009). Yet, alendronate (amino-bisphosphonate) shows an adverse effect by inhibiting the occurrence of osteoclasts by driving the osteoclasts to apoptosis at high doses (Kennel & Drake, 2009; Rosen, 2019). Hence, cytotoxicity seen in high APA or low and mid concentrations of ALE may be the sign of the osteoclast inhibition. Therefore, for the gene delivery, the lower concentration of polymer, non-toxic 5 µg/ml concentration was used to facilitate bone targeting and bone regeneration without causing any cell death at this stage of the study.

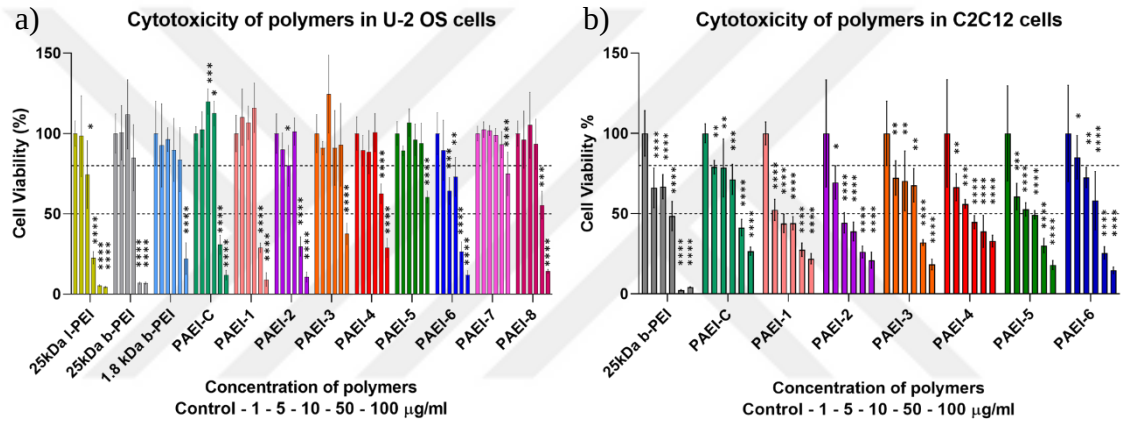

Figure 2.2. Cytotoxicity of PAEI polymers *in vitro* study, a) in U-2 OS osteosarcoma cells, b) in C2C12 myoblast cells. Data were presented as mean ± SD of independent experiments (n = 5). $p < 0.0332$ (*), $p < 0.0021$ (**), $p < 0.0002$ (***), and $p < 0.0001$(****). Dashed lines show the 80% and 50% viability.

The (bis)phosphonic acid functionalization of the cationic polymer could have reduced the charge density and decreased the cytotoxicity of the PEI. In the literature, the cytotoxicity of the PAA polymers functionalized with different groups such as ornithine (Kumar et al., 2010), acetic anhydride and benzoyl chloride (Piest & Engbersen, 2010), were reported either as polyplexes (Lin & Engbersen, 2008) or after a short incubation time of the cells with the polymers (Almulathanon et al., 2018). The slightly increased cytotoxicity of the produced polymers in this study might be a result of the incubation of polymers without plasmid and the much longer, 48 hours incubation time on the cells during cytotoxicity studies.

The myoblast muscle cells (C2C12) showed more sensitivity to both high molecular weight branched PEI and PAEI polymers than the U-2 OS cells but tolerated PAEIs better (Figure 2.2b). Viability of C2C12 cells were 48% at 10 µg/ml 25 kDa bPEI but 41% with 50 µg/ml PAEI-C. Phosphonic acid functionalization showed an adverse effect on C2C12 cell viability. Increasing the APA ratio of the polymer composition caused an increase in cytotoxicity of the polymer (PAEI-4 to PAEI-6). Alendronate addition showed the same effect as seen in U-2 OS cells (PAEI-1 to PAEI-3). At low polymer concentrations (5 to 10 µg/ml), the viability increased with increasing ALE content in the PAEIs (PAEI-1 to PAEI-3). However, at the high concentration viability of cells treated with PAEIs are all comparable and dramatically higher than cells treated with 25 kDa bPEI. For the sake of comparison, all the transfection studies were conducted at the polymer dose of 5 µg/ml.

2.5.2 Characterization of polyplexes

Complete complexation of polymers and plasmid was confirmed through gel retardation assay. Agarose gel images show no plasmid line or high molecular weight plasmid, confirming that all the plasmids were encapsulated with the PAEI polymers (Figure 2.3). However, migration of plasmid from PAEI-7 polyplex indicates that the plasmid is free and not in complex with the polymer.

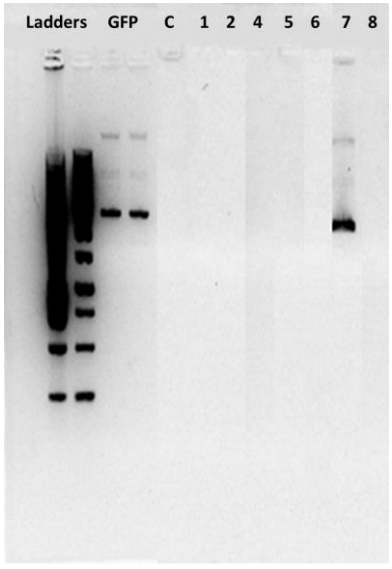

Figure 2.3. Gel retardation assay with important PAEIs in 1:10 DNA:polymer (w/w) ratio.

Hydrodynamic size of the polyplexes were measured in in OPTI-MEM® since that was the medium to be used in complex formation and transfection studies. Polyplexes were around 200-300 nm in size with 0.2-0.4 PDI (polydispersity index), while free polymers had about 1-10 nm hydrodynamic diameter and about 0.6-0.8 PDI (Figure 2.4). All the 1:4 PAA: PEI containing PAEI polymers (PAEI-1 to PAEI-6) displayed a slightly negative or nearly neutral charge, both alone and polyplex form, as seen from the zeta potentials (Figure 2.4b). The zeta potential of the high ratio of PEI containing polymers was measured as slightly negative which may confirm the micellization and negatively charged (bis)phosphonic acid effect on the surface. However, since all measurements are made in OPTI-MEM, negative zeta potential of tested samples are understandable.

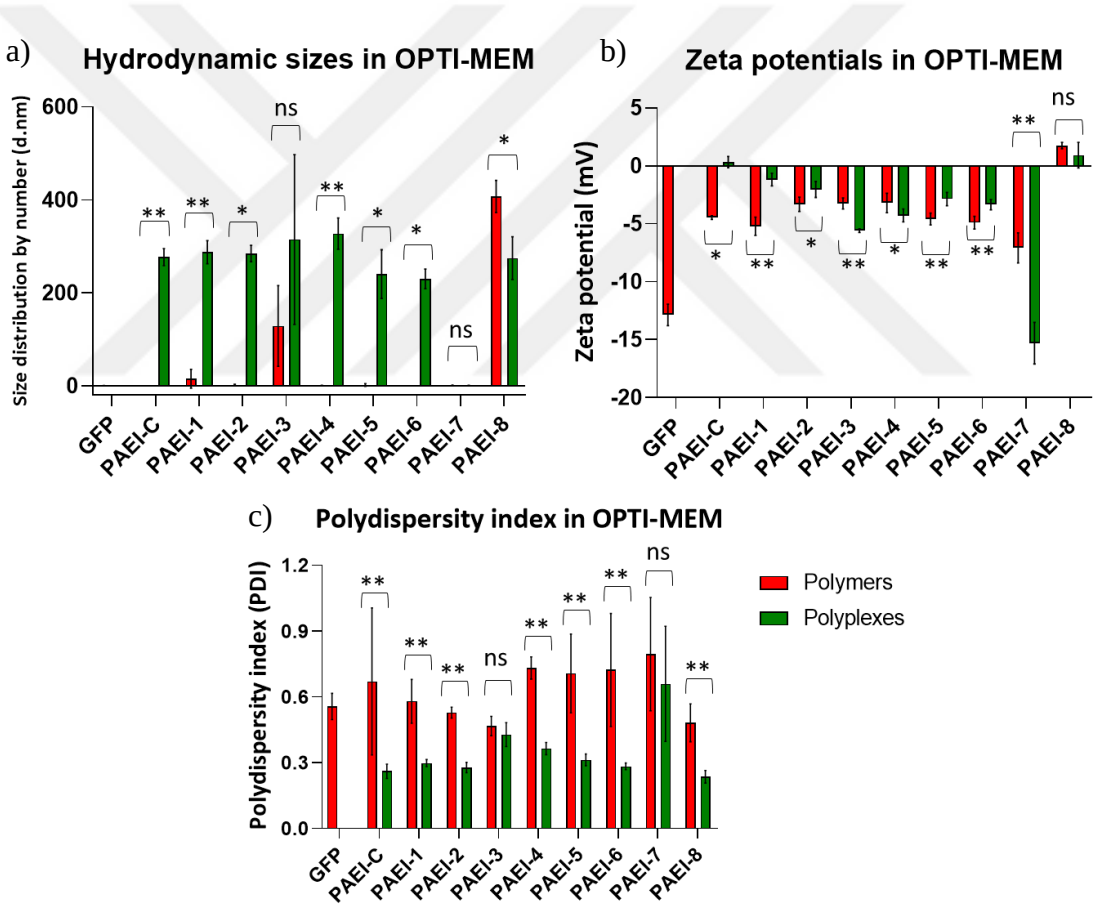

Figure 2.4. Hydrodynamic size, zeta potential and polydispersity index of polymers and polyplexes in OPTI-MEM®. a) Hydrodynamic size by number (d. nm), b) Zeta potential (mV) and c) polydispersity index. Data were presented as mean ± SD of independent experiments (n = 5). $p < 0.0332$ (*) and $p < 0.0021$ (**). n.s.: not significant.

The complex formation observed in the gel retardation assay was observed as an increase in size distribution and a significant decrease in polydispersity (Figure 2.4). Complexation of plasmid and polymers formed a relatively aggregated polyplex as may be expected with narrower size distribution.

In the case of PAEI-7, which does not contain PEI, the polydispersity index and sizes did not change significantly after the addition of plasmid and indicated a lack of complex formation. The inability of PAEI-7 to complex with the GFP plasmid was also evident in the gel retardation assay (Figure 2.3). While there is no visible plasmid band observable with any of the PAEI polymers, a plasmid band is clearly observed with PAEI-7, indicating that the plasmid is free and not in complex with the polymer.

2.5.3 Transfection of U-2 OS and C2C12 cells by using PAEI-GFP polyplexes

The gene transfection efficiency of the PAEI polymers in an osteosarcoma cell line (U-2 OS) was visualized by fluorescence microscopy (Figure 2.5) and quantified by FACS (Table 2.2) The commercial transfection agent FuGENE® was chosen as a positive control due to its exceptional efficiency in the hard-to-transfect U-2 OS cell line. 25 kDa branched PEI was also used as a positive control.

Fluorescence microscopy images reveal that although the 25 kDa PEI affords a certain level of transfection of the GFP plasmid into U-2 OS cells, the control polymer PAEI-C, which is a combination of PAA and a short-chain bPEI at a 1:4 ratio, leads to the higher efficiency of transfection (Figure 2.5). According to FACS studies, transfection efficiency was 4.87 % with 25 kDa bPEI and 11.99 % with PAEI-C (Table 2.2), indicating a more than two-fold increase in transfection.

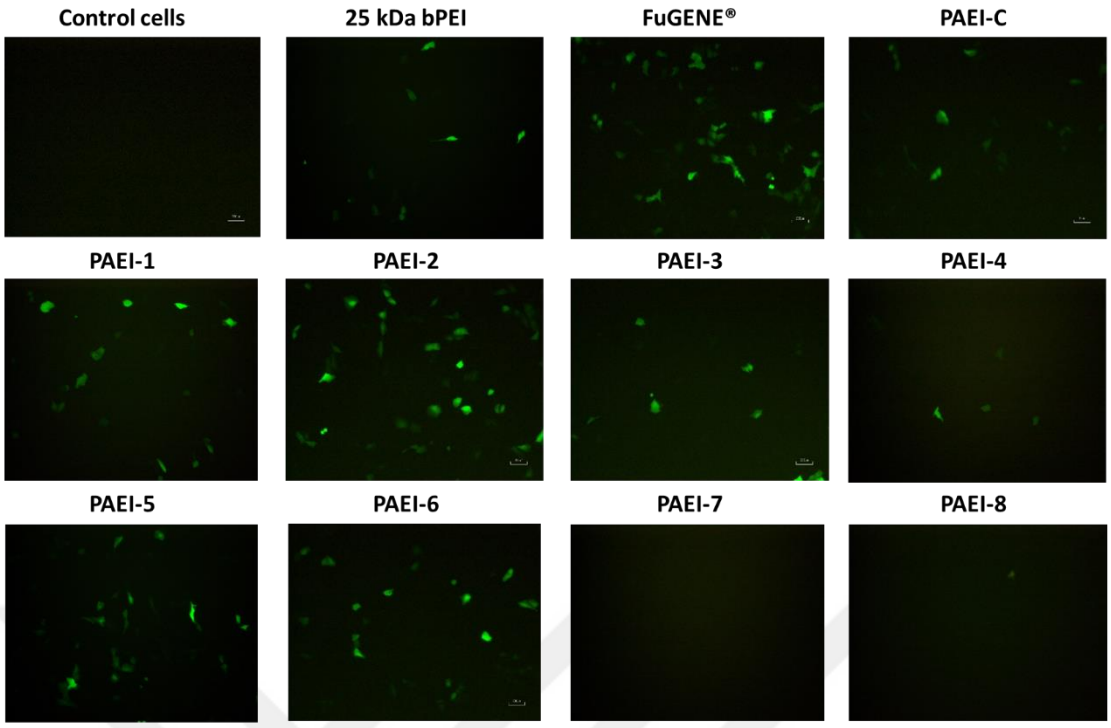

Figure 2.5. Fluorescence microscopy images of transfected U-2 OS cells with GFP plasmid complexed with a dose of 5 µg/ml of the corresponding polymer, under 10X magnification. Scale bar: 200 µm.

It should be kept in mind that many previous studies (Cavuslar et al., 2018; Fischer, Bieber, Li, Elsasser, & Kissel, 1999), show that low molecular weight PEIs of less than 10 kDa, have not been able to transfer the gene due to the low number of positively charged amines and without 1800 Da bPEI, PAEIs produced here did not form polyplex with GFP plasmid. Hence, a clear synergy resulting from the unique composition is demonstrated here.

No transfection was observed with PAEI-7 due to lack of PEI component in the composition which prevented gene binding (Figure 2.3). PAEI-8 has 1:2 PAA: PEI ratio and binds GFP as shown by the gel retardation assay. Lack of transfection indicates inefficient release.

When APA was introduced to the polymer composition, PAEI-5 with 30% of the AP of PAEI-C replaced with APA, transfection efficiency was comparable to 25kDa bPEI. At equal ratios of AP: APA (0.5: 0.5), the transfection efficiency of the polymer (PAEI-6) was as high as PAEI-C (Figure 2.5 and Table 2.2).

On the other hand, ALE addition caused a dramatic improvement in transfection efficiency. PAEI-1 with 10% ALE showed a comparable transfection efficiency to the

PAEI-6. The highest transfection efficiency with the PAEI polymers was obtained with PAEI-2, which is composed of a 0.7: 0.3 ratio of AP: ALE. Based on FACS analysis, the transfection efficiency of PAEI-2 is 26.18 %, nearly as high as that of the commercial reagent FuGENE®, which has a transfection efficiency of 27.74 % (Table 2.2) and about 5 times higher than that of 25 kDa bPEI 4.87 %.

Although in previous studies a transfection efficiency similar to 25 kDa PEI was considered successful at a 10:1 polymer: DNA (w/w) ratio using chitosan derived polymers (~100 kDa) (Kean et al., 2005), our study reveals that the PAEI polymers are at least as efficient as PEI, and can be fine-tuned to increase the transfection efficiency 5-fold.

Table 2.2. FACS study in U-2 OS cells with critical polymers in 1:10 DNA:polymer (w/w) ratio.

	% Transfection (10 000 cells)
Control cells	0.02
FuGENE®	27.74
25 kDa bPEI	4.87
PAEI-C	11.99
PAEI-2	26.18
PAEI-3	7.65
PAEI-5	5.91
PAEI-6	11.74

In C2C12 cells, a similar trend was observed, although with significantly reduced transfection efficiencies (Figure 2.6). The transfection efficiency of FuGENE® was much lower compared to U-2 OS cells. This effect was expected and is most probably due to the controlled metabolism of the normal muscle cells (Kalyanaraman, 2017). Transfection efficiency with both 25 kDa bPEI and PAEI-C was almost non-existent. With both phosphonic acid-containing polymers (PAEI-4 to PAEI-6) and alendronate-containing polymers (PAEI-1 to PAEI-3), only a few transfected cells were observed, revealing a very low overall transfection efficiency. Not only the number of transfected cells but also the intensity of the green fluorescence signal was much lower as compared to the intensity observed with U-2 OS cells.

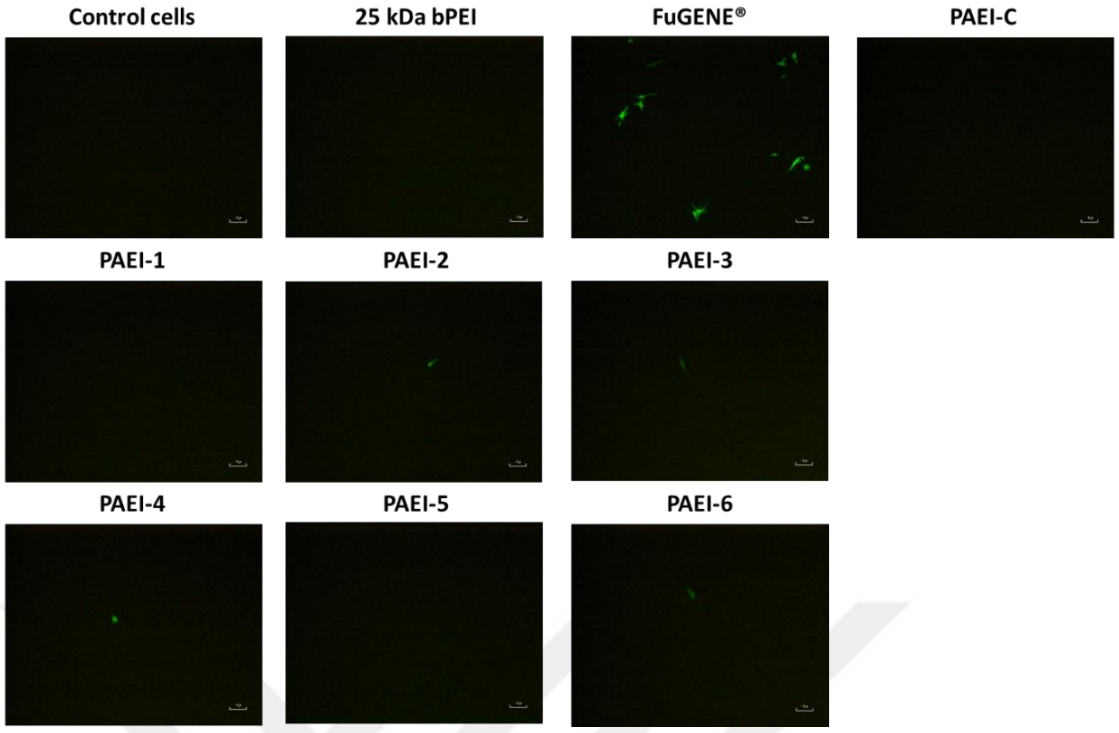

Figure 2.6. Fluorescence microscopy images of transfected C2C12 cells with GFP plasmid complexed with a dose of 5 µg/ml of the corresponding polymer, under 10X magnification. Scale bar: 200 µm.

The diminished transfection efficiency in the muscle cell line suggests that upon systemic delivery of the PAEI polymers into an organism, they will preferentially transfect the osteosarcoma cells but not the nearby healthy muscle cells. The best transfection in U-2 OS cells was observed with PAEI-2, a 30% ALE functionalized PAEI polymer. Since it is known that ALE accumulates primarily in the bone tissues (Kim et al., 2004), the presence of ALE in PAEI-2 will provide an added advantage toward targeting the PAEI-2 to the bone tissues, and enhancing the transfection efficiency further.

2.6 Conclusion

In this study, novel cytotoxicity and osteosarcoma cell transfection efficiency of PAEI polymers functionalized with phosphonic acid (APA) and alendronate (ALE) containing group in addition to 5-amino-1-pentonal (AP) was determined and the effect of these functional groups on the transfection efficiency of the formed PAEI polymers and toxicity was determined as a function of (bis)phosphonic acid content in 2D cell cultures. All PAEI polymers were able to complex the GFP plasmid, and successfully deliver the gene into the cells with at least a similar or higher efficiency than 25 kDa

bPEI. In addition, the PAEI polymers displayed decreased cytotoxicity compared to both linear and branched 25 kDa PEI (Figure 2.2). Alendronate and phosphonic acid functionalized PAEI polymers slightly increased the cytotoxicity but also increased the transfection efficiency as compared to 25 kDa bPEI. The best transfection into the tested osteosarcoma cell line, U-2 OS, was observed with alendronate (ALE) containing PAEIs. The presence of PEI, PAA, AP and ALE seem to play a complex effect in terms of both toxicity, plasmid complexation and transfection efficiency, and the best synergy was observed in the 0.7: 0.3 AP: ALE containing polymer (PAEI-2), that is comprised of a 1:4 PAA: PEI ratio, providing 26% transfection efficiency similar to FuGENE® which lacks bone targeting component. The decreased transfection in the healthy muscle cells C2C12 indicates that upon future systemic administration of PAEI-2 into the organism, it is likely to deliver the gene into the osteosarcoma cells, and not to the nearby muscle tissues, and provide selective gene therapy. The presence of alendronate on PAEI-2 will also aid in its systemic transportation to the bone tissues. Although systemic administration and organism studies were out of the scope of this work, we present a promising candidate for a novel gene delivery vehicle that can potentially be used in the treatment studies of osteosarcoma.

2.7 Acknowledgement

This study was funded by TUBITAK (grand number 117Z330; PI: Prof Avcı Semiz) and was a collaboration between Koç University and Boğaziçi University. The polymers were designed by Prof. Duygu Avcı Semiz and synthesized by Seçkin Altuncu and Melek Naz Güven at Boğaziçi University. I would like to acknowledge Dr. Yeliz Utku Konca (Koç University) for help and supervision on gene delivery experiments. I would like to thank Dr. Buse Cevatemre and Batuhan Kalkan (KUTTAM) for their help in plasmid purification.

Chapter 3:Perspectives for Future Studies

In ALA-based photodynamic therapy of colorectal cancer cells, the effective dose and irradiation procedure determined in 3D late cell structures, was critical in adaptation of this process to nanoparticle based delivery of ALA in 3D *in vitro* and *in vivo* models, which is the second part of the collaborative project funded by TUBITAK and BC. In this study, 3D cell cultures were studied for the first time in our laboratory, and the effect of the complexity on results were significant. Yet, 3D studies and AB use is quite pricy. Hence, although many *in vitro* studies may be conducted in 2D, before animal studies, testing the doses and irradiation procedure for in 3D late model is highly recommended. Noticed interaction of 5FU/ALA, which negatively effects PDT has critical value in combination therapy. The mechanism may be investigated further by isolating the 5FU/ALA complex and analysing by NMR to understand the type of reaction taking place between the two. This should be a critical warning for future combination therapies of ALA with chemotherapy agents.

The novel gene delivery vesicles were functionalized with (bis)phosphonic acid for the osteosarcoma targeted-gene delivery. ALE-containing PAEI-2 showed the transfection efficiency as much as the commercial reagent FuGENE® in 2D. The main advantage of these new polymers would be the bone targeting which should be tested *in vivo* by the follow up studies.

Chapter 4:Publications of the Author

- Buz, P. T., Duman, F. D., Erkisa, M., Demirci, G., Ari, F., Ulukaya, E. and Acar, H. Y. (2019). "Development of near-infrared region luminescent N-acetyl-L-cysteine-coated Ag_2S quantum dots with differential therapeutic effect." *Nanomedicine* **14**(8): 969 - 988.
- Duman, F. D., Akkoc, Y., Demirci, G., Bavili, N., Kiraz, A., Gozuacik, D. and Acar, H. Y. (2019). "Bypassing pro-survival and resistance mechanisms of autophagy in EGFR-positive lung cancer cells by targeted delivery of 5FU using theranostic Ag_2S quantum dots." *J Mater Chem B* **7**(46): 7363-7376.
- Guven, M. N., Demirci, G., Altuncu, S., Gulyuz, U., Okay, O., Acar, H. Y. and Avci, D. (2020). "Alendronate-functionalized poly(amido amine) cryogels of high-toughness for biomedical applications." *Polymer* **190**.
- Altuncu, S., Akyol, E., Guven, M. N., Demirci, G., Acar, H. Y. and Avci, D. (2020). "Phosphonic acid-functionalized poly(amido amine) macromers for biomedical applications." *J Biomed Mater Res A*.

Bibliography

Abedi-Gaballu, F., Dehghan, G., Ghaffari, M., Yekta, R., Abbaspour-Ravasjani, S., Baradaran, B., . . . Hamblin, M. R. (2018). PAMAM dendrimers as efficient drug and gene delivery nanosystems for cancer therapy. *Appl Mater Today, 12*, 177-190. doi:10.1016/j.apmt.2018.05.002

Allison, R. R., Downie, G. H., Cuenca, R., Hu, X.-H., Childs, C. J. H., & Sibata, C. H. (2004). Photosensitizers in clinical PDT. *Photodiagnosis and Photodynamic Therapy, 1*(1), 27-42. doi:10.1016/s1572-1000(04)00007-9

Almulathanon, A. A. Y., Ranucci, E., Ferruti, P., Garnett, M. C., & Bosquillon, C. (2018). Comparison of Gene Transfection and Cytotoxicity Mechanisms of Linear Poly(amidoamine) and Branched Poly(ethyleneimine) Polyplexes. *Pharm Res, 35*(4), 86. doi:10.1007/s11095-017-2328-7

Ashrafizadeh, M., Zarrabi, A., Hushmandi, K., Hashemi, F., Hashemi, F., Samarghandian, S., & Najafi, M. (2020). MicroRNAs in cancer therapy: Their involvement in oxaliplatin sensitivity/resistance of cancer cells with a focus on colorectal cancer. *Life Sci*, 117973. doi:10.1016/j.lfs.2020.117973

Benito-Miguel, M., Blanco, M. D., & Gomez, C. (2015). Assessment of sequential combination of 5-fluorouracil-loaded-chitosan-nanoparticles and ALA-photodynamic therapy on HeLa cell line. *Photodiagnosis Photodyn Ther, 12*(3), 466-475. doi:10.1016/j.pdpdt.2015.05.001

Bhawalkar, J. D., Kumar, N. D., Zhao, C. F., & Prasad, P. N. (1997). Two-Photon Photodynamic Therapy. *Journal of Clinical Laser Medicine & Surgery, 15*(5), 201-204.

Blake, E., & Curnow, A. (2010). The Hydroxypyridinone Iron Chelator CP94 Can Enhance PpIX-induced PDT of Cultured Human Glioma Cells. *Photochemistry and Photobiology, 86,* 1154-1160. doi:10.1111/j.1751-1097.2010.00770.x

Bonnier, F., Keating, M. E., Wrobel, T. P., Majzner, K., Baranska, M., Garcia-Munoz, A., . . . Byrne, H. J. (2015). Cell viability assessment using the Alamar blue assay: a comparison of 2D and 3D cell culture models. *Toxicol In Vitro, 29*(1), 124-131. doi:10.1016/j.tiv.2014.09.014

Borralho, P. M., Kren, B. T., Castro, R. E., da Silva, I. B., Steer, C. J., & Rodrigues, C. M. (2009). MicroRNA-143 reduces viability and increases sensitivity to 5-fluorouracil in HCT116 human colorectal cancer cells. *FEBS J, 276*(22), 6689-6700. doi:10.1111/j.1742-4658.2009.07383.x

Braun, C. S., Vetro, J. A., Tomalia, D. A., Koe, G. S., Koe, J. G., & Middaugh, C. R. (2005). Structure/function relationships of polyamidoamine/DNA dendrimers as gene delivery vehicles. *J Pharm Sci, 94*(2), 423-436. doi:10.1002/jps.20251

Bredell, M. G., Besic, E., Maake, C., & Walt, H. (2010). The application and challenges of clinical PD-PDT in the head and neck region: a short review. *J Photochem Photobiol B, 101*(3), 185-190. doi:10.1016/j.jphotobiol.2010.07.002

Buettner, G. R. (2013). Molecular Targets of Photosensitization. *Free Radical and Radiation Biology & ESR Facility*.

Bunke, A., Zerbe, O., Schmid, H., Burmeister, G., Merkle, H. P., & Gander, B. (2000). Degradation Mechanism and Stability of 5-Aminolevulinic Acid. *Journal of Pharmaceutical Sciences, 89*(10), 1335-1341. doi:10.1002/1520-6017(200010)89:103.0.CO;2-#

Cavuslar, O., Celaloglu, C., Duman, F. D., Konca, Y. U., Yagci, M. B., & Yagci Acar, H. (2018). pH and molecular weight dependence of auric acid reduction by polyethylenimine and the gene transfection efficiency of cationic gold

nanoparticles thereof. *New Journal of Chemistry, 42*(12), 10078-10083. doi:10.1039/c8nj00628h

Choi, Y. J., Kang, S. J., Kim, Y. J., Lim, Y. B., & Chung, H. W. (2010). Comparative studies on the genotoxicity and cytotoxicity of polymeric gene carriers polyethylenimine (PEI) and polyamidoamine (PAMAM) dendrimer in Jurkat T-cells. *Drug Chem Toxicol, 33*(4), 357-366. doi:10.3109/01480540903493507

Christensen, L. V., Chang, C.-W., Kim, W. J., & Kim, S. W. (2006). Reducible Poly(amido ethylenimine)s Designed for Triggered Intracellular Gene Delivery. *Bioconjugate Chem., 17*(5), 1233 - 1240.

Conry, R. M., Rodriguez, M. G., & Pressey, J. G. (2016). Zoledronic acid in metastatic osteosarcoma: encouraging progression free survival in four consecutive patients. *Clin Sarcoma Res, 6*, 6. doi:10.1186/s13569-016-0046-2

Coue, G., Freese, C., Unger, R. E., Kirkpatrick, C. J., Pickl, K. E., Sinner, F. M., & Engbersen, J. F. (2013). Design and physicochemical characterization of poly(amidoamine) nanoparticles and the toxicological evaluation in human endothelial cells: applications to peptide delivery to the brain. *J Biomater Sci Polym Ed, 24*(8), 957-971. doi:10.1080/09205063.2012.727378

De Angelis, P. M., Fjell, B., Kravik, K. L., Haug, T., Tunheim, S. H., Reichelt, W., . . . Stokke, T. (2004). Molecular characterizations of derivatives of HCT116 colorectal cancer cells that are resistant to the chemotherapeutic agent 5-fluorouracil. *International Journal of Oncology, 24*, 1279-1288.

de Freitas, C. F., Kimura, E., Rubira, A. F., & Muniz, E. C. (2020). Curcumin and silver nanoparticles carried out from polysaccharide-based hydrogels improved the photodynamic properties of curcumin through metal-enhanced singlet oxygen effect. *Mater Sci Eng C Mater Biol Appl, 112*, 110853. doi:10.1016/j.msec.2020.110853

de Oliveira Silva, F. R., Bellini, M. H., Tristao, V. R., Schor, N., Vieira, N. D., Jr., & Courrol, L. C. (2010). Intrinsic fluorescence of protoporphyrin IX from blood samples can yield information on the growth of prostate tumours. *J Fluoresc, 20*(6), 1159-1165. doi:10.1007/s10895-010-0662-9

Deng, J. Z., Sun, Y. X., Wang, H. Y., Li, C., Huang, F. W., Cheng, S. X., . . . Zhang, X. Z. (2011). Poly(beta-amino amine) cross-linked PEIs as highly efficient gene vectors. *Acta Biomater, 7*(5), 2200-2208. doi:10.1016/j.actbio.2011.02.003

Digiacomo, L., Palchetti, S., Pozzi, D., Amici, A., Caracciolo, G., & Marchini, C. (2018). Cationic lipid/DNA complexes manufactured by microfluidics and bulk self-assembly exhibit different transfection behavior. *Biochem Biophys Res Commun, 503*(2), 508-512. doi:10.1016/j.bbrc.2018.05.016

Dolmans, D. E. J. G. L., Fukumura, D., & Jain, R. K. (2003). Photodynamic Therapy for Cancer. *Nat Rev Cancer, 3*(5), 380-387. doi:10.1038/nrc1070

Dougherty, T. J., Gomer, C. J., & Henderson, B. W. (1998). Photodynamic Therapy. *Journal of the National Cancer Institute, 90*(12), 889-905.

Emilitri, E., Ferruti, P., Annunziata, R., & Ranucci, E. (2007). Novel Amphoteric Cystine-Based Poly(amidoamine)s Responsive to Redox Stimuli. *Macromolecules, 40*, 4785-4793.

Eskiler, G. G., Ozkan, A. D., Kucukkara, E. S., Kamanli, A. F., Gunoglu, B., & Yildiz, M. Z. (2020). Optimization of 5-aminolevulinic acid-based photodynamic therapy protocol for breast cancer cells. *Photodiagnosis Photodyn Ther*, 101854. doi:10.1016/j.pdpdt.2020.101854

Evans, C. L. (2015). Three-dimensional in vitro cancer spheroid models for photodynamic therapy: strengths and opportunities. *Frontiers in Physics, 3*. doi:10.3389/fphy.2015.00015

Feng, L., Hu, X., Xie, A., Yu, H., Liu, Y., Zhang, J., & Dong, W. (2015). Cationic Charged Polymer Vesicles from Amphiphilic PEI-g-PSSA-g-PEI as Potential Gene Delivery Vehicles. *Australian Journal of Chemistry, 68*(5). doi:10.1071/ch14350

Ferruti, P. (2013). Poly(amidoamine)s: Past, present, and perspectives. *Journal of Polymer Science Part A: Polymer Chemistry, 51*(11), 2319-2353. doi:10.1002/pola.26632

Ferruti, P., Franchini, J., Bencini, M., & Ranucci, E. (2007). Prevailingly Cationic Agmatine-Based Amphoteric Polyamidoamine as a Nontoxic, Nonhemolytic, and "Stealthlike" DNA Complexing Agent and Transfection Promoter. *Biomacromolecules, 8*, 1498 - 1504.

Ferruti, P., Marchisio, M. A., & Duncan, R. (2002). Poly(amido-amine)s: Biomedical Applications. *Macromol. Rapid Commun., 23*, 332 - 355.

Fischer, D., Bieber, T., Li, Y., Elsasser, H., & Kissel, T. (1999). A Novel Non-Viral Vector for DNA Delivery Based on Low Molecular Weight, Branched Polyethylenimine: Effect of Molecular Weight on Transfection Efficiency and Cytotoxicity. *Pharmaceutical Research, 16*(8), 1273-1279.

Frame, F. M., Savoie, H., Bryden, F., Giuntini, F., Mann, V. M., Simms, M. S., . . . Maitland, N. J. (2016). Mechanisms of growth inhibition of primary prostate epithelial cells following gamma irradiation or photodynamic therapy include senescence, necrosis, and autophagy, but not apoptosis. *Cancer Med, 5*(1), 61-73. doi:10.1002/cam4.553

Godbey, W. T., Kenneth, K. W., & Mikos, A. G. (1999). Tracking the intracellular path of poly(ethylenimine)/DNA complexes for gene delivery. *Proc. Natl. Acad. Sci., 96*, 5177-5181.

Gold, M. H., & Goldman, M. P. (2004). 5-Aminolevulinic Acid Photodynamic Therapy: Where We Have Been and Where We are Going. *Dermatol Surg., 30*(8), 1077-1084.

Gu, W., Wu, C., Chen, J., & Xiao, Y. (2013). Nanotechnology in the targeted drug delivery for bone diseases and bone regeneration. *Int J Nanomedicine, 8*, 2305-2317. doi:10.2147/IJN.S44393

Hamid, R., Rotshteyn, Y., Rabadi, L., Parikh, R., & Bullock, P. (2004). Comparison of alamar blue and MTT assays for high through-put screening. *Toxicol In Vitro, 18*(5), 703-710. doi:10.1016/j.tiv.2004.03.012

Hatakeyama, T., Murayama, Y., Komatsu, S., Shiozaki, A., Kuriu, Y., Ikoma, H., . . . Otsuji, E. (2013). Efficacy of 5-aminolevulinic acid-mediated photodynamic therapy using light-emitting diodes in human colon cancer cells. *Oncol Rep, 29*(3), 911-916. doi:10.3892/or.2013.2220

Howells, L. M., Sale, S., Sriramareddy, S. N., Irving, G. R., Jones, D. J., Ottley, C. J., . . . Brown, K. (2011). Curcumin ameliorates oxaliplatin-induced chemoresistance in HCT116 colorectal cancer cells in vitro and in vivo. *Int J Cancer, 129*(2), 476-486. doi:10.1002/ijc.25670

Huang, R., Ke, W., Liu, Y., Jiang, C., & Pei, Y. (2008). The use of lactoferrin as a ligand for targeting the polyamidoamine-based gene delivery system to the brain. *Biomaterials, 29*(2), 238-246. doi:10.1016/j.biomaterials.2007.09.024

Inoue, K., Karashima, T., Kamada, M., Shuin, T., Kurabayashi, A., Furihata, M., . . . Sasaki, J. (2009). Regulation of 5-aminolevulinic acid-mediated protoporphyrin

IX accumulation in human urothelial carcinomas. *Pathobiology, 76*(6), 303-314. doi:10.1159/000245896

Jones, N. A., Hil, I. R. C., Stolnik, S., Bignotti, F., Davis, S. S., & Garnett, M. C. (2000). Polymer chemical structure is a key determinant of physicochemical and colloidal properties of polymer^DNA complexes for gene delivery. *Biochimica et Biophysica Acta*, 1-18.

Juzeniene, A., Juzenas, P., Ma, L. W., Iani, V., & Moan, J. (2004). Effectiveness of different light sources for 5-aminolevulinic acid photodynamic therapy. *Lasers Med Sci, 19*(3), 139-149. doi:10.1007/s10103-004-0314-x

Kalyanaraman, B. (2017). Teaching the basics of cancer metabolism: Developing antitumor strategies by exploiting the differences between normal and cancer cell metabolism. *Redox Biol, 12*, 833-842. doi:10.1016/j.redox.2017.04.018

Kean, T., Roth, S., & Thanou, M. (2005). Trimethylated chitosans as non-viral gene delivery vectors: cytotoxicity and transfection efficiency. *J Control Release, 103*(3), 643-653. doi:10.1016/j.jconrel.2005.01.001

Kennedy, J. C., Marcus, S. L., & Pottier, R. H. (1996). Photodynamic Therapy (PDT) and Photodiagnosis (PD) Using Endogenous Photosensitization Induced by 5-Aminolevulinic Acid (ALA): Mechanisms and Clinical Results. *Journal of Clinical Laser Medicine & Surgery, 14*(5), 289-304.

Kennel, K. A., & Drake, M. T. (2009). Adverse Effects of Bisphosphonates: Implications for Osteoporosis Management. *Mayo Clin. Proc., 84*(7), 632-638.

Khdair, A., Chen, D., Patil, Y., Ma, L., Dou, Q. P., Shekhar, M. P., & Panyam, J. (2010). Nanoparticle-mediated combination chemotherapy and photodynamic therapy overcomes tumor drug resistance. *J Control Release, 141*(2), 137-144. doi:10.1016/j.jconrel.2009.09.004

Khot, M. I., Perry, S. L., Maisey, T., Armstrong, G., Andrew, H., Hughes, T. A., . . . Jayne, D. G. (2018). Inhibiting ABCG2 could potentially enhance the efficacy of hypericin-mediated photodynamic therapy in spheroidal cell models of colorectal cancer. *Photodiagnosis Photodyn Ther, 23*, 221-229. doi:10.1016/j.pdpdt.2018.06.027

Kim, T., Seo, H. J., Choi, J. S., Jang, H., Baek, J., Kim, K., & Park, J. (2004). PAMAM-PEG-PAMAM: Novel Triblock Copolymer as a Biocompatible and Efficient Gene Delivery Carrier. *Biomacromolecules, 5*, 2587-2592.

Krieg, R. C., Messmann, H., Rauch, J., Seeger, S., & Knuechel, R. (2002). Metabolic Characterization of Tumor Cell–specific Protoporphyrin IX Accumulation After Exposure to 5-Aminolevulinic Acid in Human Colonic Cells¶. *Photochemistry and Photobiology, 76*(5). doi:10.1562/0031-8655(2002)076<0518:Mcotcs>2.0.Co;2

Kumar, A., Yellepeddi, V. K., Davies, G. E., Strychar, K. B., & Palakurthi, S. (2010). Enhanced gene transfection efficiency by polyamidoamine (PAMAM) dendrimers modified with ornithine residues. *Int J Pharm, 392*(1-2), 294-303. doi:10.1016/j.ijpharm.2010.03.054

La-Beck, N. M., Liu, X., Shmeeda, H., Shudde, C., & Gabizon, A. A. (2019). Repurposing amino-bisphosphonates by liposome formulation for a new role in cancer treatment. *Semin Cancer Biol*. doi:10.1016/j.semcancer.2019.12.001

Lavignac, N., Lazenby, M., Foka, P., Malgesini, B., Verpilio, I., Ferruti, P., & Duncan, R. (2004). Synthesis and endosomolytic properties of poly(amidoamine) block copolymers. *Macromol Biosci, 4*(10), 922-929. doi:10.1002/mabi.200400093

Lee, J. H., Lim, Y., Choi, J. S., Lee, Y., Kim, T., Kim, H. J., . . . Park, J. (2003). Polyplexes Assembled with Internally Quaternized PAMAM-OH Dendrimer and Plasmid

DNA Have a Neutral Surface and Gene Delivery Potency. *Bioconjugate Chem., 14*(6), 1214-1221. doi:10.1021/bc034095g

Li, Y., Xiao, P., Huang, Z., Chen, X., Yan, X., Zhai, J., & Ma, Y. (2020). Evaluation of curcumin-mediated photodynamic therapy on the reverse of multidrug resistance in tumor cells. *RSC Advances, 10*(1), 298-306. doi:10.1039/c9ra09996d

Lin, C., & Engbersen, J. F. (2008). Effect of chemical functionalities in poly(amido amine)s for non-viral gene transfection. *J Control Release, 132*(3), 267-272. doi:10.1016/j.jconrel.2008.06.022

Lin, C., Zhong, Z., Lok, M. C., Jiang, X., Hennink, W. E., Feijen, J., & Engbersen, J. F. J. (2007). Novel Bioreducible Poly(amido amine)s for Highly Efficient Gene Delivery. *Bioconjugate Chem., 18*, 138 - 145.

Lipton, A. (2008). Emerging role of bisphosphonates in the clinic--antitumor activity and prevention of metastasis to bone. *Cancer Treat Rev, 34 Suppl 1*, S25-30. doi:10.1016/j.ctrv.2008.03.008

Loschenov, V. B., Konov, V. I., & Prokhorov, A. M. (2000). Photodynamic Therapy and Fluorescence Diagnostics. *Laser Physics, 10*(6), 1188-1207.

Macdonald, I. J., & Dougherty, T. J. (2001). Basic principles of photodynamic therapy. *J. Porphyrins Phthalocyanines, 5*, 105-129.

Manfredi, A., Ranucci, E., Suardi, M., & Ferruti, P. (2016). Polymerization Kinetics of Poly(amidoamine)s in Different Solvents. *Journal of Bioactive and Compatible Polymers, 22*(2), 219-231. doi:10.1177/0883911507076453

Martinez-Negro, M., Sanchez-Arribas, N., Guerrero-Martinez, A., Moya, M. L., Tros de Ilarduya, C., Mendicuti, F., . . . Junquera, E. (2019). A Non-Viral Plasmid DNA Delivery System Consisting on a Lysine-Derived Cationic Lipid Mixed with a Fusogenic Lipid. *Pharmaceutics, 11*(12). doi:10.3390/pharmaceutics11120632

Meyerhardt, J. A., & Mayer, R. J. (2005). Systemic Therapy for Colorectal Cancer. *N Engl J Med, 352*, 476-487.

Moghimi, S. M., Symonds, P., Murray, J. C., Hunter, A. C., Debska, G., & Szewczyk, A. (2005). A two-stage poly(ethylenimine)-mediated cytotoxicity: implications for gene transfer/therapy. *Mol Ther, 11*(6), 990-995. doi:10.1016/j.ymthe.2005.02.010

Mohammad-Hadi, L., MacRobert, A. J., Loizidou, M., & Yaghini, E. (2018). Photodynamic therapy in 3D cancer models and the utilisation of nanodelivery systems. *Nanoscale, 10*(4), 1570-1581. doi:10.1039/c7nr07739d

Mroz, P., Yaroslavsky, A., Kharkwal, G. B., & Hamblin, M. R. (2011). Cell death pathways in photodynamic therapy of cancer. *Cancers (Basel), 3*(2), 2516-2539. doi:10.3390/cancers3022516

O'Brien, J., Wilson, I., Orton, T., & Pognan, F. (2000). Investigation of the Alamar Blue (resazurin) fluorescent dye for the assessment of mammalian cell cytotoxicity. *Eur. J. Biochem., 267*, 5421-5426.

Ohashi, S., Kubo, T., Ikeda, T., Arai, Y., Takahashi, K., Hirasawa, Y., . . . Mazda, O. (2001). Cationic polymer-mediated genetic transduction into cultured human chondrosarcoma-derived HCS-2/8 cells. *J Orthop Sci, 6*, 75-81.

Ohba, T., Cole, H. A., Cates, J. M., Slosky, D. A., Haro, H., Ando, T., . . . Schoenecker, J. G. (2014). Bisphosphonates inhibit osteosarcoma-mediated osteolysis via attenuation of tumor expression of MCP-1 and RANKL. *J Bone Miner Res, 29*(6), 1431-1445. doi:10.1002/jbmr.2182

Oleinick, N. L. (2011). Basic Photosensitization. *Department of Radiation Oncology - Case Western Reserve University School of Medicine*.

Pack, D. W., Hoffman, A. S., Pun, S., & Stayton, P. S. (2005). Design and development of polymers for gene delivery. *Nat Rev Drug Discov, 4*(7), 581-593. doi:10.1038/nrd1775

Peng, L., Gao, Y., Xue, Y. N., Huang, S. W., & Zhuo, R. X. (2010). Cytotoxicity and in vivo tissue compatibility of poly(amidoamine) with pendant aminobutyl group as a gene delivery vector. *Biomaterials, 31*(16), 4467-4476. doi:10.1016/j.biomaterials.2010.02.031

Peng, Q., Warloe, T., Berg, K., Moan, J., Kongshaug, M., Giercksky, K., & Nesland, J. M. (1997). 5-Aminolevulinic Acid-Based Photodynamic Therapy. *American Cancer Society, 79*(12), 2282-2308.

Piest, M., & Engbersen, J. F. J. (2010). Effects of charge density and hydrophobicity of poly(amido amine)s for non-viral gene delivery. *J Control Release, 148*(1), 83-90. doi:10.1016/j.jconrel.2010.07.109

Pignatello, R., Cenri, E., Micieli, D., Fotia, C., Salerno, M., Granchi, D., . . . Baldini, N. (2009). A novel biomaterial for osteotropic drug naocarriers: synthesis and biocompatibility evaluation of a PLGA-ALE conjugate. *Nanomedicine, 4*(2), 161-175. doi:10.2217/17435889.4.2.161

Pramual, S., Lirdprapamongkol, K., Jouan-Hureaux, V., Barberi-Heyob, M., Frochot, C., Svasti, J., & Niamsiri, N. (2020). Overcoming the diverse mechanisms of multidrug resistance in lung cancer cells by photodynamic therapy using pTHPP-loaded PLGA-lipid hybrid nanoparticles. *Eur J Pharm Biopharm, 149*, 218-228. doi:10.1016/j.ejpb.2020.02.012

Rampersad, S. N. (2012). Multiple applications of Alamar Blue as an indicator of metabolic function and cellular health in cell viability bioassays. *Sensors (Basel), 12*(9), 12347-12360. doi:10.3390/s120912347

Rawla, P., Sunkara, T., & Barsouk, A. (2019). Epidemiology of colorectal cancer: incidence, mortality, survival, and risk factors. *Prz Gastroenterol, 14*(2), 89-103. doi:10.5114/pg.2018.81072

Richardson, S. C. W., Pattrick, N. G., Man, Y. K. S., Ferruti, P., & Duncan, R. (2001). Poly(Amidoamine)s as Potential Nonviral Vectors: Ability to Form Interpolyelectrolyte Complexes and to Mediate Transfection in Vitro. *Biomacromolecules, 2*, 1023-1028.

Rodriguez, L., Batlle, A., Di Venosa, G., MacRobert, A. J., Battah, S., Daniel, H., & Casas, A. (2006). Study of the mechanisms of uptake of 5-aminolevulinic acid derivatives by PEPT1 and PEPT2 transporters as a tool to improve photodynamic therapy of tumours. *Int J Biochem Cell Biol, 38*(9), 1530-1539. doi:10.1016/j.biocel.2006.03.002

Rosen, H. N. (2019). Pharmacology of bisphosphonates (Review).

Sayles, L. C., Breese, M. R., Koehne, A. L., Leung, S. G., Lee, A. G., Liu, H. Y., . . . Sweet-Cordero, E. A. (2019). Genome-Informed Targeted Therapy for Osteosarcoma. *Cancer Discov, 9*(1), 46-63. doi:10.1158/2159-8290.CD-17-1152

Siegel, R. L., Miller, K. D., Goding Sauer, A., Fedewa, S. A., Butterly, L. F., Anderson, J. C., . . . Jemal, A. (2020). Colorectal cancer statistics, 2020. *CA Cancer J Clin, 70*(3), 145-164. doi:10.3322/caac.21601

Subbiah, V., Wagner, M. J., McGuire, M. F., Sarwari, N. M., Devarajan, E., Lewis, V. O., . . . Anderson, P. (2015). Personalized comprehensive molecular profiling of high risk osteosarcoma: Implications and limitations for precision medicine. *Oncotarget, 6*(38), 40642-40654.

Sun, M., Iqbal, J., Singh, S., Sun, L., & Zaidi, M. (2010). The crossover of bisphosphonates to cancer therapy. *Ann N Y Acad Sci, 1211*, 107-112. doi:10.1111/j.1749-6632.2010.05812.x

Sun, Y., Xian, L., Yu, J., Yang, T., Zhang, J., Yang, Z., . . . Ding, P. (2017). Structure-Function Correlations of Poly(Amido Amine)s for Gene Delivery. *Macromol Biosci, 17*(3). doi:10.1002/mabi.201600297

Tahmasebi, H., Khoshgard, K., Sazgarnia, A., Mostafaie, A., & Eivazi, M. T. (2016). Enhancing the efficiency of 5-aminolevulinic acid-mediated photodynamic therapy using 5-fluorouracil on human melanoma cells. *Photodiagnosis Photodyn Ther, 13*, 297-302. doi:10.1016/j.pdpdt.2015.08.011

Tan, M. L., Choong, P. F., & Dass, C. R. (2009). Osteosarcoma: Conventional treatment vs. gene therapy. *Cancer Biol Ther, 8*(2), 106-117. doi:10.4161/cbt.8.2.7385

Triesscheijn, M., Baas, P., Schellens, J. H., & Stewart, F. A. (2006). Photodynamic therapy in oncology. *Oncologist, 11*(9), 1034-1044. doi:10.1634/theoncologist.11-9-1034

Ullah, I., Muhammad, K., Akpanyung, M., Nejjari, A., Neve, A. L., Guo, J., . . . Shi, C. (2017). Bioreducible, hydrolytically degradable and targeting polymers for gene delivery. *J Mater Chem B, 5*(18), 3253-3276. doi:10.1039/c7tb00275k

Vader, P., van der Aa, L. J., Engbersen, J. F., Storm, G., & Schiffelers, R. M. (2012). Physicochemical and biological evaluation of siRNA polyplexes based on PEGylated Poly(amido amine)s. *Pharm Res, 29*(2), 352-361. doi:10.1007/s11095-011-0545-z

Wachowska, M., Muchowicz, A., Firczuk, M., Gabrysiak, M., Winiarska, M., Wańczyk, M., . . . Golab, J. (2011). Aminolevulinic Acid (ALA) as a Prodrug in Photodynamic Therapy of Cancer. *Molecules, 16*(5), 4140-4164. doi:10.3390/molecules16054140

Wan, C., Qian, J., Li, F., & Li, H. (2015). Ultrasound-targeted microbubble destruction enhances polyethylenimine-mediated gene transfection in vitro in human retinal pigment epithelial cells and in vivo in rat retina. *Mol Med Rep, 12*(2), 2835-2841. doi:10.3892/mmr.2015.3703

Wawrzyniec, K., Kawczyk-Krupka, A., Czuba, Z. P., Krol, W., & Sieron, A. (2015). The influence of ALA-mediated photodynamic therapy on secretion of selected growth factors by colon cancer cells in hypoxia-like environment in vitro. *Photodiagnosis Photodyn Ther, 12*(4), 598-611. doi:10.1016/j.pdpdt.2015.11.001

Yang, X., Palasuberniam, P., Kraus, D., & Chen, B. (2015). Aminolevulinic Acid-Based Tumor Detection and Therapy: Molecular Mechanisms and Strategies for Enhancement. *Int J Mol Sci, 16*(10), 25865-25880. doi:10.3390/ijms161025865

Zanoni, M., Piccinini, F., Arienti, C., Zamagni, A., Santi, S., Polico, R., . . . Tesei, A. (2016). 3D tumor spheroid models for in vitro therapeutic screening: a systematic approach to enhance the biological relevance of data obtained. *Sci Rep, 6*, 19103. doi:10.1038/srep19103

Zhang, H., & Vinogradov, S. V. (2010). Short biodegradable polyamines for gene delivery and transfection of brain capillary endothelial cells. *J Control Release, 143*(3), 359-366. doi:10.1016/j.jconrel.2010.01.020

Zinselmeyer, B. H., Mackay, S. P., Schatzlein, A. G., & Uchegbu, I. F. (2002). The Lower-Generation Polypropylenimine Dendrimers Are Effective Gene-Transfer Agents. *Pharmaceutical Research, 19*(7), 960-967.